A Mathematical Model of a Vibrating Soil-Foundation System

By G. F. WEISSMANN

(Manuscript received October 8, 1965)

The displacement amplitudes and the phase angles of vertically vibrating rigid circular plates on an elastic isotropic homogeneous half-space have been expressed in terms of the mass of the plate, the static spring constant multiplied by a frequency-dependent function, and a damping term. The results have been modified to apply to vibrating soil-foundation systems. The effects of hysteresis damping, nonlinear load-deflection characteristics of soils, the static prepressure, the change of soil properties with depth, and the difference between static and dynamic stress-strain relations of soils have been considered. The mathematical model has been compared with data on vibrations of circular foundations. The agreement between the model and the experimental data for cohesive soils is very good.

I. INTRODUCTION

Numerous attempts have been made to develop a mathematical model capable of representing the steady-state vibrations of a soil-foundation system. E. Reissner[1] solved the problem of vertical vibrations of a rigid circular plate on a semi-infinite elastic solid. A sign error in his work was discovered by O. J. Šechter[2] who presented also a corrected analytical solution for this case. T. Y. Sung[3] continued this work for different pressure distributions between the plate and the solid. G. N. Bycroft[4] presented approximate solutions of the steady-state vibrations for the degrees of freedom of a rigid circular plate on an elastic isotropic half-space and on an elastic stratum. Since the mathematical solutions become rather difficult, this approach has been used only for a strongly idealized soil, namely the semi-infinite elastic isotropic solid. Another approach to this problem is the determination of a simplified mathematical model capable of describing the vibrations of a soil-foundation system. O. J. Šechter[2] showed that the amplitude-frequency response curve of a vibrating system consisting of constant mass, viscous damping force, and linear spring constant differs only slightly from that

caused by vertical vibrations of a circular plate on an elastic half-space, provided the mass of the plate is multiplied by a factor and the damping coefficient is chosen appropriately. This approach has been extended by M. Novák[5,6] who introduced a frequency independent nonlinear restoring force. G. Ehlers[7] attempted to simulate the soil-foundation system by assuming the foundation to be supported by a truncated pyramid of soil. This approach was used also by A. Pauw,[8] and H. A. Balakrishna Rao and C. N. Nagaraj.[9] However, none of the above mentioned models was capable of representing the amplitude-frequency response curves of several soil-foundation systems investigated by R. K. Bernhard and J. Finelli,[10] who concluded that an equivalent system could not be analogous to a simple spring-mass system with viscous damping and linear elasticity.

The purpose of this paper is to present a quasilinear system sufficiently adaptable to represent the amplitude-frequency response and phase angle-frequency curves of circular foundations on soil.

II. THE VIBRATIONS OF CIRCULAR FOUNDATIONS ON AN ELASTIC HALF-SPACE*

The vertical steady-state vibrations of circular foundations on a homogeneous elastic isotropic half-space have been investigated analytically by E. Reissner,[1] O. J. Šechter,[2] T. Y. Sung,[3] and G. N. Bycroft.[4] According to their work the displacement amplitude becomes

$$y_0 = \frac{F_0}{Gr_0}\sqrt{\frac{f_1^2 + f_2^2}{(1 + b_0a_0^2f_1)^2 + (b_0a_0^2f_2)^2}}. \tag{1}$$

The phase angle is

$$\tan \Phi = -\frac{f_2}{f_1 + b_0a_0^2(f_1^2 + f_2^2)}, \tag{2}$$

where

y_0 = displacement amplitude of foundation,
F_0 = force amplitude of harmonic exciting force,
G = shear modulus of half-space,
r_0 = radius of circular foundation,
$b_0 = m_0/\rho r_0^3$ = mass ratio,
m_0 = mass of circular foundation,
ρ = mass density of half-space,
$a_0 = r_0\omega\sqrt{\rho/G_s}$ = frequency factor,

* The letter symbols used in this paper are defined where they first appear and are arranged alphabetically, for convenience or reference, in the Appendix.

Φ = phase angle between exciting force and displacement,
G_s = dynamic shear modulus of half-space,
ω = angular frequency,
f_1 and f_2 are functions of the dimensionless frequency factor a_0, of Poisson's ratio ν of the half-space and of the assumed pressure distribution between the half-space and the foundation.

T. Y. Sung[3] determined the functions f_1 and f_2 for different contact pressure distributions and different Poisson's ratios in terms of power series of the frequency factor a_0 for $a_0 \leqq 1.5$. The values of these functions for a pressure distribution caused by a rigid circular plate are shown in Fig. 1. The functions f_1 and f_2 as determined by G. N. Bycroft[4] differ somewhat from those used in this paper which are based on T. Y. Sung's[3] work. It should be noted that for zero frequency, f_1 approaches a finite value and f_2 becomes equal to zero.

For zero frequency, (1) becomes

$$y_{os} = -\frac{F_0}{Gr_0} f_{10} \tag{3}$$

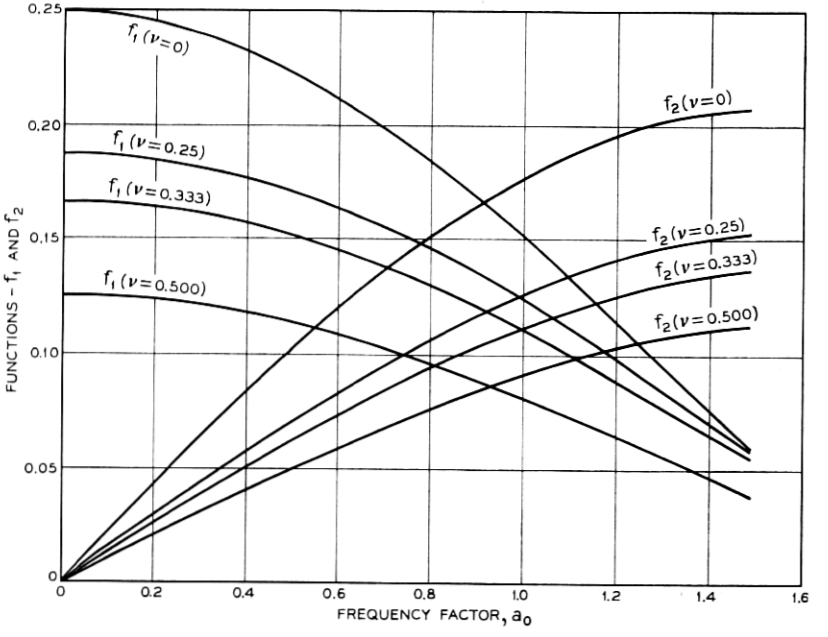

Fig. 1 — Functions f_1 and f_2 for rigid circular plates.

where

$y_{0s} = \lim_{\omega \to 0} y_0$ = displacement of foundation due to static load F_0, and

$f_{10} = \lim_{a_0 \to 0} f_1$ = value of f_1 for zero frequency.

From Fig. 1 it follows that the value of f_{10} can be expressed as

$$-f_{10} = \frac{1 - \nu}{4}. \tag{4}$$

Substituting (4) in (3) results in an expression for the displacement of a rigid circular plate on a homogeneous elastic half-space due to a vertical static force. This expression is identical to that derived by Boussinesq[11] in 1885.

It is readily verified that (1) and (2) can be written as

$$y_0 = \frac{F_0}{\sqrt{[C_s\alpha - m_0\omega^2]^2 + [C_s\beta]^2}} \tag{5}$$

$$\tan \Phi = \frac{C_s\beta}{C_s\alpha - m_0\omega^2} \tag{6}$$

where

$$C_s = -\frac{Gr_0}{f_{10}} = \frac{4Gr_0}{1 - \nu} = \lim_{\omega \to 0} \frac{F_0}{y_0} \tag{7}$$

$$\alpha = \frac{f_1 f_{10}}{f_1^2 + f_2^2} = -\frac{1 - \nu}{4} \frac{f_1}{f_1^2 + f_2^2} \tag{8}$$

$$\beta = -\frac{f_2 f_{10}}{f_1^2 + f_2^2} = \frac{1 - \nu}{4} \frac{f_2}{f_1^2 + f_2^2}. \tag{9}$$

C_s represents the static spring constant of a rigid circular plate on an elastic isotropic homogeneous half-space. Its magnitude depends on the shear modulus and Poisson's ratio of the half-space and on the radius of the rigid plate.

α and β are functions of the frequency factor a_0 and of Poisson's ratio ν as shown in Fig. 2. They have been computed using the values of f_1 and f_2 shown in Fig. 1. The values of the functions α and β for $\nu = 0$ and $\nu = \frac{1}{3}$ are plotted in Fig. 2 only, because the values for $\nu = \frac{1}{4}$ and $\nu = \frac{1}{2}$ fall between those shown. Since $a_0 = r_0\omega\sqrt{\rho/G_s}$, the functions α and β depend on the magnitude of the radius of the plate, r_0, the frequency, ω, the dynamic shear modulus, G_s, of the half-space, and the mass-density ρ, of the half-space.

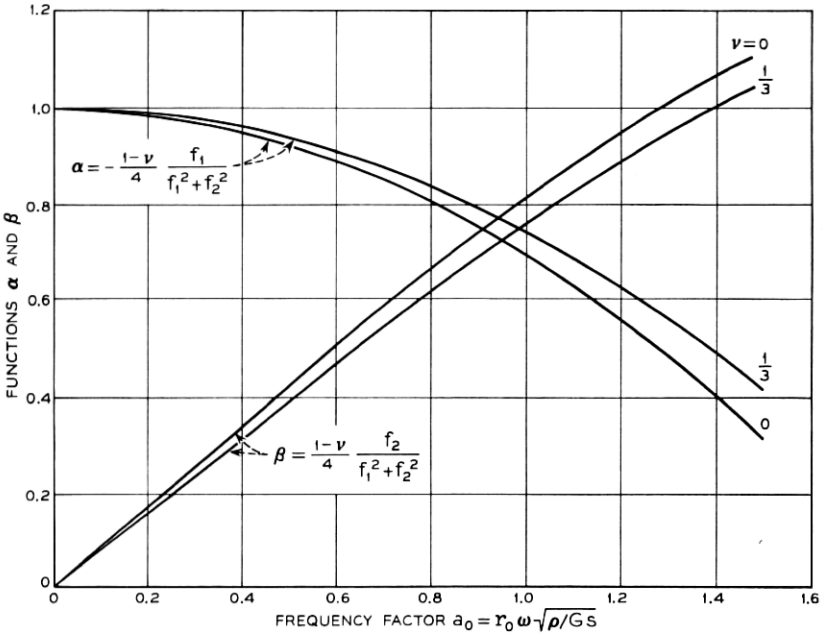

Fig. 2 — Functions α and β vs frequency factor a_0 .

The square root of the ratio of the dynamic shear modulus, G_s, to the mass-density, ρ, represents the shear wave velocity, v_s,

$$v_s = \sqrt{\frac{G_s}{\rho}} . \tag{10}$$

It should be mentioned that, for many materials, the dynamic shear modulus, G_s , as obtained from wave velocity measurements, is larger than the shear modulus, G, determined by means of static or slow dynamic tests.

For large shear wave velocities, the function α approaches one and β approaches zero. For this case, (5) represents the displacement amplitude and (6) the phase angle of a linear vibrating system without damping. This system consists of the mass of the plate, a weightless spring with a spring constant defined by (7), and a harmonic exciting force. It becomes apparent that the functions α and β modify this simple system to account for the additional effect of the mass-density of the half-space.

The functions α and β, as shown in Fig. 2, can be expressed with

sufficient accuracy as follows:

$$\alpha = 1 - \varepsilon a_0^2 = 1 - \varepsilon \left(\frac{r_0}{v_s}\right)^2 \omega^2 \tag{11}$$

$$\beta = b_1 a_0 = b_1 \left(\frac{r_0}{v_s}\right) \omega \tag{12}$$

where ε and b_1 are appropriately selected constants. The values of ε and b_1 depend on Poisson's ratio; ε varies between 0.26 and 0.30, and β between 0.76 and 0.85.

III. THE PARTICIPATING MASS OF THE HALF-SPACE

H. Lorenz[12] introduced the concept of the participating soil mass in order to explain some results of foundation vibration tests. O. J. Šechter[2] proved that the vertical vibration of a circular plate on an elastic half-space can be expressed, with sufficient accuracy, by means of a constant mass, a viscous damping force, and a spring constant. The mass consists of the mass of the plate, m_0, multiplied by a factor which accounts for the mass of the half-space vibrating in-phase with the plate. The displacement amplitudes and the phase angles of such a system can be written as

$$y_0 = \frac{F_0}{\sqrt{[C_s - \bar{m}\omega^2]^2 + [b\omega]^2}} \tag{13}$$

$$\tan \Phi = \frac{b\omega}{C_s - \bar{m}\omega^2} \tag{14}$$

where

$\bar{m} = m_0 + m_s$ = constant mass,
m_s = participating mass of half-space, and
b = damping constant.

Equations (13) and (14) are identical to (5) and (6), provided the constant mass and the damping constant are selected as follows:

$$\bar{m} = m_0 \left[1 + \varepsilon \frac{C_s}{m_0} \left(\frac{r_0}{v_s}\right)^2\right] \tag{15}$$

$$b = b_1 \frac{r_0}{v_s} C_s . \tag{16}$$

This identity is readily shown by substitution of (15) and (16) in (13) and (14).

IV. DYNAMIC STIFFNESS

Some investigators, such as W. Heukelom,[13,14] expressed the results of foundation vibration tests in terms of the dynamic stiffness and the phase angle. The dynamic stiffness is defined as the ratio of the force amplitude between the foundation and the subsoil to the resulting displacement amplitudes. The steady-state vibrations of a rigid circular plate on an elastic half-space shall now be expressed in these terms.

The force acting at the surface of the half-space can be expressed as

$$\bar{F} = F - m_0 \ddot{y} \tag{17}$$

where

$\bar{F} = \bar{F}_0 e^{i(\omega t + \Psi)}$ = force acting between plate and half-space,
$\bar{F}_0$ = force amplitude acting between plate and half-space,
Ψ = phase angle between $\bar{F}$ and the resulting displacement,
$F = F_0 e^{i(\omega t + \Phi)}$ = exciting force acting on plate,
$y = y_0 e^{i\omega t}$ = displacement of plate,
$\ddot{y} = -y_0 \omega^2 e^{i\omega t}$ = acceleration of plate,
Φ = phase angle between F and the resulting displacement,
$i = \sqrt{-1}$.

The force amplitude acting between the plate and the half-space becomes

$$\bar{F}_0 = \sqrt{F_0^2 + 2F_0 m_0 y_0 \omega^2 \cos \Phi + (m_0 y_0 \omega^2)^2} \tag{18}$$

and for the phase angle between the force acting at the surface of the half-space and the displacement, the following expression is obtained:

$$\tan \Psi = \frac{F_0 \sin \Phi}{F_0 \cos \Phi + m_0 y_0 \omega^2}. \tag{19}$$

The dynamic stiffness is defined as the ratio of the force amplitude acting between the plate and the half-space and the resulting displacement amplitude and becomes, by means of (18),

$$S = \frac{\bar{F}_0}{y_0} = \frac{F_0}{y_0} \sqrt{1 + 2 \frac{m_0 y_0}{F_0} \omega^2 \cos \Phi + \left(\frac{m_0 y_0 \omega^2}{F_0} \right)^2} \tag{20}$$

where

S = dynamic stiffness.

Substituting y_0 and Φ, expressed by means of (5) and (6), in (20), the dynamic stiffness becomes

$$S = C_s \sqrt{\alpha^2 + \beta^2} \tag{21}$$

and by substitution of (5) and (6) in (19), the following expression is

obtained for the phase angle Ψ:

$$\tan \Psi = \frac{\beta}{\alpha}. \tag{22}$$

Substitution of the values for α and β from Fig. 2 or of the approximate expression for α and β given by (11) and (12) in (21) shows that the dynamic stiffness of the half-space is essentially equal to the static stiffness or the static spring constant, C_s. The effect of α and β on the dynamic stiffness is negligibly small.

Substitution of α and β in (22) shows that the phase angle between the force acting at the surface of the half-space and the displacement remains always smaller than 90 degrees for values of the frequency factor, a_0, smaller or equal to 1.5.

V. DAMPING

Energy propagation to infinity provides the only damping of the vibrations of a rigid circular plate on an ideally elastic homogeneous half-space. The energy dissipated per cycle becomes

$$D_s = \oint F \, dy \tag{23}$$

where

D_s = dissipated energy per cycle,
$F = F_0 \sin (\omega t + \Phi)$,
$y = y_0 \sin \omega t$.

By substitution of (5) and (6) in (23) the following is obtained:

$$D_s = \pi C_s \beta y_0^2. \tag{24}$$

The energy required for the deformation of the half-space becomes

$$U_s = \tfrac{1}{2} C_s \alpha y_0^2 \tag{25}$$

where

U_s = energy required for the deformation of the half-space.

It should be noted that the energy required for the deformation of the half-space is equal to the maximum energy stored in the half-space reduced by the inertia effects of the half-space.

The loss coefficient of the circular plate on the ideally elastic half-space shall be defined as

$$\eta_s = \frac{D_s}{2\pi U_s} = \frac{\beta}{\alpha} \tag{26}$$

where

η_s = loss coefficient of vibrating circular plate.

The loss coefficient of the circular plate on the elastic half-space should be identical to the phase angle between the force amplitude acting between the plate and the half-space and the resulting displacement amplitude shown in (22).

It should be pointed out that both the dissipated energy and the energy of the half-space are proportional to the static spring constant C_s. The loss coefficient of the vibrating system, however, is a function of α and β alone. α and β are defined by means of (8) and (9). Equations (11) and (12) are approximate expressions of α and β.

The medium of the half-space was considered to be ideally elastic and hence, the propagation of energy to infinity provided the only source of energy dissipation. However, engineering materials and particularly soils are not ideally elastic but dissipate energy due to internal friction if subjected to cyclic stresses. The author and R. R. Hart[15] determined the specific damping capacity or the coefficient of energy absorption of some granular soils by means of laboratory tests. The specific damping capacity is defined as the amount of energy absorbed by a unit volume of the material per unit of energy spent for deformation per cycle. The specific damping capacity for these granular soils varied between 0.4 and 0.9. D. D. Barkan[16] reported values between 0.64 and 0.79 for sand. For clayey soils the damping capacity varied between 0.2 and 0.6. Furthermore, it was established that the specific damping capacity of sandy and clayey soils does not depend on the rate of stress application, the frequency of changes in the stress, the maximum alternating stress, or the static prestresses. The loss coefficient is obtained by division of the specific damping capacity by 2π.

$$\eta = \frac{\Psi_0}{2\pi} \tag{27}$$

where

η = loss coefficient of material

Ψ_0 = specific damping capacity of material.

The loss coefficient, η, is considered to be a basic property of a material. The difference between the loss coefficient of a material, η, and the loss coefficient of a vibrating system, η_s, should be noted.

G. N. Bycroft[4] investigated the effect of internal friction of the medium of the half-space on the functions f_1 and f_2 shown in Fig. 1. f_1 becomes numerically smaller and f_2 greater for small values of the frequency factor, a_0. Changes of f_1 and f_2 affect the function α and β shown

in Fig. 2 and defined by means of (8) and (9). The effect of such a change on the function α is rather small and α can still be expressed, with sufficient accuracy, by means of (11). The function β becomes approximately

$$\beta = \eta + b_1 a_0 = \eta + b_1 \frac{r_0 \omega}{v_s}. \tag{28}$$

For small values of the frequency factor, a_0, or for high shear wave velocities and small radii of the plates, the effect of the loss coefficient of the medium becomes significant.

An approximate expression of the loss coefficient of the vibrating circular plate is obtained by substitution of (11) and (28) in (26)

$$\eta_s = \frac{\eta + b_1 a_0}{1 - \varepsilon a_0^2} = \frac{\eta + b_1 \left(\frac{r_0 \omega}{v_s}\right)}{1 - \varepsilon \left(\frac{r_0 \omega}{v_s}\right)^2}. \tag{29}$$

For zero frequency, the loss coefficient of the plate becomes equal to the loss coefficient of the medium of the half-space. This is true only if the loss coefficient of the material is independent of the magnitude of the applied static and cyclic stresses. The author[17] measured the loss coefficient of circular plates on clayey silt subjected to slowly alternating loads. The results varied between 0.1 and 0.15. Considering the additional friction between the plate and the soil, the results agree well with those obtained by laboratory tests of sandy and clayey soils as reported by the author[15] and by D. D. Barkan.[16]

VI. NONLINEAR RESTORING FORCE

The static spring constant of a rigid circular plate on an elastic isotropic homogeneous half-space has been expressed by means of (7). For this idealized medium, the deflection is a single-valued linear function of the applied force. For engineering materials, and particularly for soils, this relationship becomes considerably more complex. Due to the effect of hysteresis damping, the deformation caused by the application of an alternating force is no longer a single-valued function. Two different forces cause the same deformation under the condition of loading and unloading. Furthermore, the average of these two forces may be a nonlinear function of the deformation and/or the rate of deformation. Other factors, such as static preloads and change of the properties of the half-space with depth, further complicate the force-deformation relation.

In view of the mathematical complexity of strongly nonlinear vibration problems, it shall be assumed that the nonlinearities of the force-displacement function within a limited range are small. For this case the nonlinear force-displacement function can be expressed with sufficient accuracy by means of an equivalent linear function.

$$F_s = f(y) \approx C_s(y_0)y \quad \text{for} \quad -y_0 \leqq y \leqq y_0 \tag{30}$$

where

$F_s = f(y)$ = nonlinear force-displacement function, and
$C_s(y_0)$ = amplitude dependent spring constant.

The spring constant, C_s, should be selected in such a manner that the stored energy at the displacement amplitude of both the nonlinear and the equivalent linear systems are equal.

$$U = \int_0^{y_0} F_s dy = \int_0^{y_0} f(y)dy = \tfrac{1}{2}C_s(y_0)y_0^2 \tag{31}$$

where

U = stored energy.

The spring constant as a function of the displacement amplitude is readily obtained by solving (31) with respect to C_s. The static spring constant can frequently be expressed by the following empirical equation:

$$C_s = C_0 y_0^{-n} \tag{32}$$

where

C_0 and n are appropriately selected constants.

It should be noted that (32) is an empirical function which has been used successfully by the author[17] to express the amplitude, dependent load-deflection characteristics of circular plates on some soils. Other functions may be more suitable to define these characteristics for different soils.

The amplitude-frequency response curves and the phase angle frequency curves of circular plates on a quasielastic homogeneous isotropic half-space with hysteresis damping are obtained by substitution of (11), (28), and (32) in (5) and (6). For the amplitude-frequency response curves, biquadratic equations of the frequency as a function of the amplitudes are obtained.

VII. THE VIBRATING SOIL-FOUNDATION SYSTEM

The load-deflection characteristics of circular rigid plates on soil are generally expressed in terms of the coefficient of subgrade reaction

which is defined as the ratio of the average applied stress to the resulting displacement. The spring constant of a rigid circular plate on soil becomes then

$$C_s = \pi r_0^2 k_s \tag{33}$$

where

k_s = coefficient of subgrade reaction.

By means of (7) and (33) the coefficient of subgrade reaction of circular rigid plates on an elastic isotropic homogeneous half-space can be expressed as

$$k_s = \frac{4G}{\pi(1 - \nu)r_0}. \tag{34}$$

For this case, the coefficient of subgrade reaction becomes inversely proportional to the radius of the plate.

The author[17] determined the coefficient of subgrade reaction of a silty clay experimentally. Circular plates of different radii, r_0, were loaded to produce various average prepressures, $\bar{p}$, between the plate and the subsoil. This static prepressure was maintained until the creep settlements of the plates became negligibly small. An average stress, $\bar{\sigma}_n$, was then repeatedly added to and subtracted from the prepressure, $\bar{p}$. The resulting displacements were measured. Fig. 3 shows the results schematically. The coefficient of subgrade reaction, k_s, is calculated by dividing the alternating stress amplitude, $\bar{\sigma}_n$, by the corresponding vertical displacement, y_n. The results may be summarized as follows:

(*i*) The coefficient of subgrade reaction decreased with an increase of the alternating stress amplitude, $\bar{\sigma}_n$.

(*ii*) An increase of the static prepressure, $\bar{p}$, caused an increase of the coefficient of subgrade reaction.

(*iii*) An increase of the radius, r_0, caused a decrease of the coefficient of subgrade reaction; however, this decrease was generally smaller than (34), valid for the elastic half-space, would indicate.

The author and S. R. White[18] have shown that the dependence of the coefficient of subgrade reaction on the static prepressure can be rather significant for some soils.

S. D. Wilson and E. A. Sibley[19] have shown that the shear modulus increases with an increase of the rate of load application. A modulus value determined from velocity measurements was almost an order of magnitude higher than that determined by means of static compression tests. Typical data reported by R. V. Whitman[20] show a similar phenomenon. Only for sands, the shear modulii obtained by seismic tests

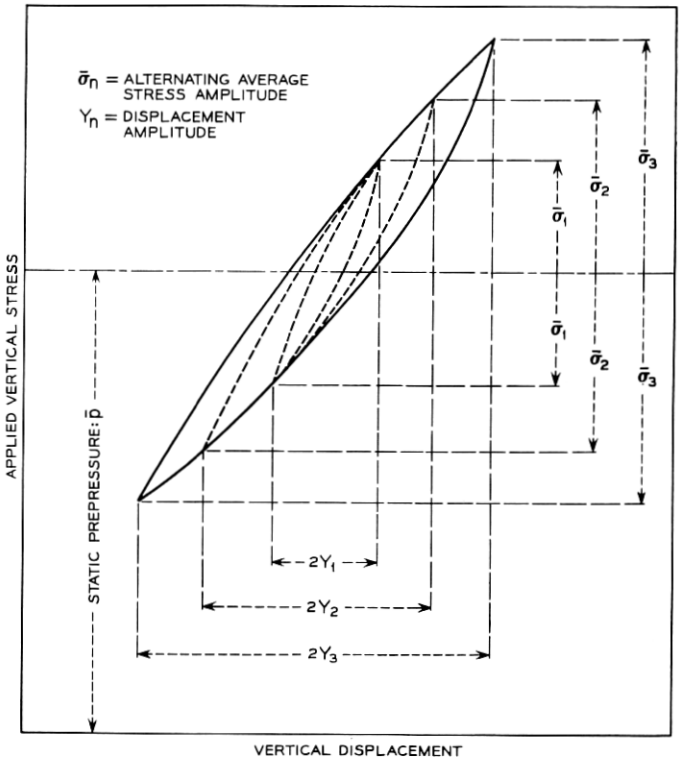

Fig. 3 — Coefficient of subgrade reaction.

did not differ much from that determined by means of static compression tests. Based on these results, it appears reasonable to assume that the coefficient of subgrade reaction of some soils increases also with an increased frequency of the load application.

Because the static prepressure, $\bar{p}$, and the radius, r_0, of the foundation are important parameters affecting the magnitude of the coefficient of subgrade reaction, k_s, the mass, m_0, of the foundation should be expressed as

$$m_0 = \frac{1}{g} \pi r_0^2 \bar{p} \tag{35}$$

where

g = acceleration of gravity.

Substituting (11), (28), (33), and (35) in (5) and (6), the following

expressions for the displacement amplitude, y_0, and the phase angle, Φ, are obtained:

$$y_0 = \frac{F_0}{\pi r_0^2 k_s \sqrt{\left[1 - \{1 + \varepsilon \bar{a}_0^2\} \frac{\bar{p}}{k_s g} \omega^2\right]^2 + \left[\eta + b_1 \frac{r_0}{v_s} \omega\right]^2}} \tag{36}$$

$$\tan \Phi = \frac{\eta + b_1 \frac{r_0}{v_s} \omega}{1 - \{1 + \varepsilon \bar{a}_0^2\} \frac{\bar{p}}{k_s g} \omega^2} \tag{37}$$

where

$$\bar{a}_0 = \frac{r_0}{v_s} \sqrt{\frac{k_s g}{\bar{p}}}. \tag{38}$$

The resonance frequency becomes

$$\omega_0 = \sqrt{\frac{k_s g}{\bar{p}\{1 + \varepsilon \bar{a}_0^2\}}} = \sqrt{\frac{k_s g}{\bar{p}\left[1 + \varepsilon \frac{r_0^2}{v_s^2} \frac{k_s g}{\bar{p}}\right]}}. \tag{39}$$

In order to estimate the magnitude of $\bar{a}_0$, (10) and (34) are substituted in (38) to yield

$$\bar{a}_0 = \frac{r_0}{v_s} \sqrt{\frac{k_s g}{\bar{p}}} = \sqrt{\frac{4\rho g G r_0}{\pi(1 - \nu) G_s \bar{p}}} = \sqrt{\frac{4\gamma r_0 G}{\pi(1 - \nu)\bar{p} G_s}} \tag{40}$$

where

$\gamma = \rho g$ = density of soil.

For most soils, with the exception of sand, the shear modulus obtained by means of slow vibration tests is smaller than that obtained by seismic velocity measurements and hence $G/G_s < 1$. The specific weight of soils, γ, is generally smaller than the average contact pressure between the foundation and the subsoil, $\bar{p}$, and therefore $\gamma/\bar{p} < 1$. Since the foundation is considered to be rigid, the magnitude of the radius, r_0, must be limited. An increase of the radius r_0 would require a corresponding increase of the average contact pressure, $\bar{p}$. Hence, it is reasonable to assume that $\bar{a}_0$ is, for many materials, a small quantity and that $\varepsilon \bar{a}_0$ is then small compared to one. For this case, (39) can be simplified to

$$\omega_0 \approx \sqrt{k_s g/\bar{p}}. \tag{41}$$

The amplitude at resonance, y_{0r}, for a constant exciting force, F_0, follows from (36)

$$y_{0r} = \frac{F_0}{\pi r_0^2 k_s \left[\eta + b_1 \frac{r_0}{v_s}\omega_0\right]} \tag{42}$$

and for a centrifugal exciting force $F_0 = m_1 e_0 \omega_0^2$ where m_1 is the eccentric mass and e_0 the eccentricity of the rotating weights:

$$y_{0r} = \frac{m_1 e_0 \omega_0^2}{\pi r_0^2 k_s \left[\eta + b_1 \frac{r_0\omega_0}{v_s}\right]} = \frac{m_1 e_0 g}{\pi r_0^2 \bar{p}} \frac{\left[1 - \varepsilon\left(\frac{r_0\omega_0}{v_s}\right)^2\right]}{\left[\eta + b_1\left(\frac{r_0\omega_0}{v_s}\right)\right]}. \tag{43}$$

The loss coefficient at resonance can be expressed by means of (29) and (43) as

$$\eta_s = \frac{\eta + b_1\left(\frac{r_0\omega_0}{v_s}\right)}{1 - \varepsilon\left(\frac{r_0\omega_0}{v_s}\right)^2} = \frac{m_1 e_0 g}{\pi r_0^2 \bar{p} y_{0r}} = \frac{m_1 e_0}{m_0 y_{0r}}. \tag{44}$$

It is now hypothesized that (36) and (37) describe the amplitude-frequency response and the phase angle-frequency relation of a rigid circular foundation on soil, provided the coefficient of subgrade reaction, k_s, the shear wave velocity, v_s, and the loss coefficient of the soil y, are determined experimentally and the constants ε and b_1 are selected according to the model of the rigid circular plate on the elastic half-space as 0.26 and 0.76, respectively. For sand, with its relatively low shear wave velocity, the term $r_0\omega_0/v_s$ may exceed 1.5 and (36) to (39) are no longer applicable.

The validity of this hypothesis can only be established by the evaluation of the data obtained by means of vibration tests.

VIII. THE EVALUATION OF VIBRATION TEST DATA

Vertical vibration tests of rigid circular foundations on soil were conducted by H. Lorenz[12,23] in Germany, D. D. Barkan[16] in the U.S.S.R., M. Novák[5,6] in Czechoslovakia, W. Heukelom[13,14] in the Netherlands, F. J. Converse[22] of California Institute of Technology, and Z. B. Fry[21] of the U. S. Army Engineer Waterways Experiment Station. R. K. Bernhard and J. Finelli[10] of Rutgers University used a rigid square foundation.

A vertical sinusoidal exciting force, F, was applied to the foundation and the resulting displacements were measured. Generally, these displacements could be expressed with sufficient accuracy in terms of a sinusoidal function.

The weight of the foundation and its dimensions are considered to be known quantities. They can be expressed in terms of the average contact pressure between the foundation and the subsoil and the radius of the foundation. In case of square foundations, the radius of an equivalent circular foundation with the same contact area as the square foundation was used.

The exciting force amplitude, F_0, is also considered to be a known function of the frequency. For all these reported tests, the exciting force has been produced by means of eccentrically rotating weights and therefore, can be expressed as $F_0 = m_1 e_0 \omega^2$.

The following experimental data can be obtained from a well conducted foundation vibration test:

(*i*) The displacement amplitude-frequency response curve, $y_0(\omega)$, and

(*ii*) The phase angle-frequency curve, $\Phi(\omega)$.

However, the measurements of the phase angle-frequency curve is relatively difficult, and a number of investigators did not determine these data. In some cases only the resonance frequency was measured.

Solving (5) and (6) with respect to $C_s\alpha$ and $C_s\beta$ the following equations are obtained:

$$C_s\alpha = \frac{F_0}{y_0}\left[\frac{m_0 y_0 \omega^2}{F_0} + \cos\Phi\right] = \pi r_0^2 k_s\alpha \tag{45}$$

$$C_s\beta = \frac{F_0}{y_0}\sin\Phi = \pi r_0^2 k_s\beta. \tag{46}$$

$k_s\alpha$ shall be defined as the "dynamic coefficient of subgrade reaction." By means of (45) and (46) it is always possible to calculate the parameters $C_s\alpha$ and $C_s\beta$, provided the mass of the foundation, m_0, is known and the force amplitude-frequency relation, $F_0(\omega)$, the displacement amplitude-frequency relation, $y_0(\omega)$, and the phase angle-frequency relation, $\Phi(\omega)$, have been determined experimentally.

Substitution of these values for $C_s\alpha$ and $C_s\beta$ back in (5) and (6) will obviously result in a perfect fit of the calculated amplitude-frequency response curve and the phase angle-frequency curve with the experimental data. However, according to (33), C_s is a function of the coefficient of subgrade reaction, k_s. The coefficient of subgrade reaction, k_s, in turn is, as discussed previously, a function of the displacement amplitude, y_0, and of the frequency, ω. Due to the large amplitude changes occurring close to the resonance frequency, even small nonlinearities of the stress-displacement relation may cause a considerable change of the

magnitude of the coefficient of subgrade reaction. From a single amplitude-frequency response curve and the corresponding phase angle-frequency curve, it is impossible to determine the effect of the displacement amplitude on the parameters $C_s\alpha$ and $C_s\beta$. However, if the exciting force amplitude is changed a number of amplitude-frequency response curves and phase angle-frequency curves are obtained, and it is possible to evaluate points of constant frequency at different displacement amplitudes or of constant displacement amplitudes at different frequencies. In this manner, the effect of frequency and amplitude on the parameters $C_s\alpha$ and $C_s\beta$ can be determined.

The loss coefficient, η_s, of the vibrating system is defined by means of (26). Substitution of (45) and (46) in (26) results in

$$\eta_s = \frac{\sin \Phi}{\left[\frac{m_0 y_0 \omega^2}{F_0} + \cos \Phi\right]}. \tag{47}$$

It should be noted that for phase angles Φ greater than $\pi/2$, the denominator in (47) becomes a difference, and small experimental errors will have a considerable effect on the calculated magnitude of the loss coefficient, η_s. Furthermore, (47) shows again that the loss coefficient does not depend on the spring constant, C_s.

If the phase angle-frequency data are not available, $C_s\alpha$ and $C_s\beta$ can be calculated from the amplitude-frequency response curve for specific frequencies only. For low frequencies, the phase angle Φ can be assumed to be approximately equal to zero, at high frequencies equal to π, and at resonance equal to $\pi/2$. Unfortunately, for a centrifugal exciting force, the displacement amplitudes at low frequencies are rather small and the data become relatively inaccurate; at high frequencies, the exciting force amplitude frequently exceeds the weight of the foundations and no data are taken. It is always possible to select frequency dependent functions in such a manner that an amplitude-frequency response curve calculated by means of (5) will fit the experimental data. This is possible for any arbitrary amplitude dependent function, $C_s(y_0)$. However, there is no physical significance in fitting one particular amplitude-frequency response curve. A mathematical model capable of describing the vibrations of a vibrating soil-foundation system should not only fit the amplitude-frequency response curve and the phase angle-frequency curve of one particular test but should also predict the effect of a change in radius, r_0, of the foundation, of a change of the static contact pressure, $\bar{p}$, and of a change of the exciting force amplitude, F_0.

IX. RESONANCE DATA OF VERTICAL STEADY-STATE VIBRATIONS OF RIGID FOUNDATIONS

A direct comparison of the data of vibrating rigid foundations shown in the literature is complicated by the different units and nomenclature used to express the results of these tests. In order to facilitate such a comparison, data obtained at resonance have been collected and are presented in Table I, using uniform units and nomenclature.

The authors of the publications used are listed in Column 2 of the table.

The type of soil is shown in Column 3.

The radius, r_0, of circular foundations is shown in Column 4 and is expressed in feet. In case of a square foundation, such as used by R. K. Bernhard and J. Finelli,[10] the radius of an equivalent circular foundation with the same contact area as the square foundation was used.

The average static contact pressure, $\bar{p}$, between the foundation and the subsoil is shown in Column 5 and is expressed in pounds per square foot.

Column 6 shows the angular resonance frequency, ω_0, expressed in radians per second. Resonance occurs if the phase angle between the exciting force and the resulting displacement is equal to $\pi/2$ or 90 degrees. For centrifugal excitation, resonance is sometimes determined by the tangent to the amplitude-frequency response curve through the origin. This is correct only for a linear damping force; however, the possible error is small. Even the difference of the frequency at maximum amplitude and the resonance frequency remains relatively small.

The exciting force amplitude, F_0, is listed in Column 7 in terms of pounds. H. Lorenz[23] and R. K. Bernhard and J. Finelli[10] reported some results for which the exciting force at resonance becomes greater than the weight of the foundation. These data are not included in Table I.

Column 8 shows the displacement amplitude at resonance in inches multiplied by 10^3.

The loss coefficient at resonance, a dimensionless quantity, is listed in Column 9 and has been calculated by means of (44).

The compression and shear wave velocities, v_c, and, v_s, are shown in Column 10 and are expressed in feet per second.

Column 11 shows the coefficient of subgrade reactions, k_s, which is defined as the ratio of the average stress caused by a static force acting on a rigid circular or square plate to the resulting displacement. The coefficient of subgrade reaction is expressed in pounds per square foot per inch.

The type of data reported by the investigators are listed in Column 12.

Table I shows clearly the need for more complete reporting of the obtained test data and of associated significant soil parameters.

Some typical values of the compression and shear wave velocities for different soils have been listed by D. D. Barkan[16] and are shown in Table II.

X. EXPERIMENTAL VERIFICATION OF THEORY

Equation (29) shall now be used to predict the loss coefficient, η_s, of vibrating rigid circular foundations. The results shall be compared with the loss coefficient, η_s, obtained by substitution of foundation vibration data in (47).

Z. B. Fry[21] of the U. S. Army Waterways Experiment Station reported the results of vibration tests of rigid circular foundations on a silty clay. Fig. 4 shows a typical amplitude-frequency response curve and the corresponding phase angle-frequency curve. An average shear wave velocity $v_s = 475$ ft/sec was determined for this soil.

Fig. 5 shows the loss coefficient, η_s, obtained by substitution of the shear wave velocity, v_s, in (29). A loss coefficient of the soil of $\eta = 0.1$ was assumed, and, based on the model of the rigid circular plate on an elastic half-space, the constants $\varepsilon = 0.26$ and $b_1 = 0.76$ were used. Furthermore, for a number of frequencies, the loss coefficient, η_s, was calculated by substitution of the data shown in Fig. 4 in (47). The agreement between the predicted and experimentally determined values of the loss coefficient is very good. The data show that the loss coefficient is affected to some degree by the magnitude of the exciting force amplitude.

The loss coefficient at resonance can be calculated by means of (44). The resonance frequencies, ω_0, and the displacement amplitudes at resonance, y_{0r}, of foundations having different radii, r_0, contact pressures, $\bar{p}$, and exciting force amplitudes, F_0, are listed in Table I. The data reported by Z. B. Fry[21] for silty clay having a shear wave velocity $v_s = 475$ ft/sec are listed from numbers H-1a to H-10d. The loss coefficients, η_s, at resonance are shown in Fig. 6 as a function of the product of radius and resonance frequency, $r_0\omega_0$. The agreement between the loss coefficient predicted by means of (29) and these experimental values is excellent.

The resonance data obtained by M. Novák are shown in Table I (A-1a to A-10c). The tests were conducted on a loess loam. The loss coefficients calculated by means of (44) are shown in Fig. 7. Unfortunately, the shear wave velocity, v_s, was not reported. Therefore, a

Table I—Resonance Data of Vertical Foundation Vibration Tests

1	2	3	4	5	6	7	8	9	10		11	12
No.	Reference	Soil	Radius of Foundation	Average Static Contact Pressure	Angular Resonance Frequency	Exciting Force Amplitude at Resonance	Displacement Amplitude at Resonance	Loss Coefficient of Soil-Foundation System at Resonance	Compression Wave Velocity	Shear Wave Velocity	Coefficient of Subgrade Reaction	Type of Available Data
			r_0 [ft]	$\bar{p}$ [lb/ft²]	ω_0 [Rad/sec]	$F_0 = m_1 e \omega_0^2$ [lb]	y_{0r} [in $\times 10^{-3}$]	η_s [—]	v_c [ft/sec]	v_s [ft/sec]	k_s [lb/ft²/in]	
A-1a	M. Novák[5]	Loess Loam	1.85	445	187	479	2.4	0.454				Amplitude-Frequency Response Curves
b					183	870	5.2	0.402				
c					173	1,515	10.0	0.406				
d					162	1,975	14.5	0.420				
e					158	1,825	14.9	0.409				
f					150	2,220	18.7	0.425				
2a				346	200	549	2.8	0.698				Resonance Frequency and Amplitude at Resonance
b					187	911	5.7	0.652				
c					171	1,475	12.4	0.581				
3a				248	210	602	3.0	0.665				
b					178	1,600	14.3	0.511				
4a			1.60	625	160	351	3.4	0.310				
b					151	578	6.6	0.301				
c					140	990	12.9	0.298				
5a			1.31	987	132	238	4.2	0.237				
b					124	402	8.6	0.220				
c					115	667	17.5	0.210				
d					113	963	24.8	0.221				
6a				692	149	304	5.1	0.277				
b					143	531	10.2	0.266				
c					132	880	21.6	0.243				
7a				397	118 / 165 ?	427	7.5	0.325				
b						708	15.8	0.298				

b					162	1,323	5.2	0.450				
c					157	1,860	6.1	0.571				
9a				379	188	584	1.6	0.552				
b					182	861	3.3	0.500				
c					170	1,460	6.9	0.456				
d					162	1,980	10.2	0.470				
10a				262	213	622	1.7	0.719				
b					205	1,095	3.7	0.640				
c					191	1,844	8.3	0.554				
B-1a	M. Novák[5]	Sandy Clay	1.85	420	203	1,070	7.9	0.281				
b					190	1,433	11.5	0.295				
c					181	1,658	14.5	0.298				
C-1	D. D. Barkan[16]	15 feet saturated clay on sand	2.61	1,670	88			0.290			22.90	
2			3.70	968	60			0.266			12.75	
3			5.23	770	69			0.362			10.68	
D-1	D. D. Barkan[16]	Soft saturated silty clay	1.30	1,335	73			0.142			18.30	
2			1.85	1,045	69			0.116			13.10	
3			2.27	916	70			0.102			10.95	
E-1	D. D. Barkan[16]	Loess	1.66	1,090	159						74.00	
2			2.19	1,550	107						56.20	
3			2.62	1,105	117						53.70	Resonance Frequency and Amplitude at Resonance
4			3.70	874	121						42.70	
F-1	D. D. Barkan[16]	Fine saturated sand	1.85	762	95						20.60	
2a			3.70	421	143						23.20	
b					181						39.30	
3			5.25	692	130						28.90	
4			7.16	490	124						20.80	
5a			1.85	1,390				0.264				
b								0.380				
c								0.350				
6				3,360				0.320				
G-1	R. K. Bernhard and J. Finelli[10]	Gravel with silt	1.50	222	188	562	14.8	0.278				Amplitude-Frequency Response Curves

TABLE I—*Continued*

1	2	3	4	5	6	7	8	9	10		11	12
No.	Reference	Soil	Radius of Foundation	Average Static Contact Pressure	Angular Resonance Frequency	Exciting Force Amplitude at Resonance	Displacement Amplitude at Resonance	Loss Coefficient of Soil-Foundation System at Resonance	Compression Wave Velocity	Shear Wave Velocity	Coefficient of Subgrade Reaction	Type of Available Data
			r_0 [ft]	$\bar{p}$ [lb/ft²]	ω_0 [Rad/sec]	$F_0 = m_1 e \omega_0^2$ [lb]	y_{0r} [in × 10^{-3}]	η_s [—]	v_c [ft/sec]	v_s [ft/sec]	k_s [lb/ft²/in]	
H-1a	Waterways Experiment Station[21]	Silty Clay	2.58	1,478	86.7	2,780	10.0	0.365	1,000	475		
b					78.5	4,540	25.2	0.361				
c					72.5	5,870	40.0	0.345				
d					70.3	7,245	69.5	0.259				
2a				1,478	90.4	3,025	10.0	0.462				
b					80.4	4,765	23.5	0.410				
c					77.9	6,720	43.0	0.321				
d					73.5	7,920	62.8	0.292				
3a				1,225	94.8	3,325	12.0	0.464				
b					85.4	5,375	28.5	0.390				
c					78.5	6,820	48.5	0.343				
d					74.1	8,055	68.3	0.324				
4a				1,225	94.2	3,285	13.8	0.404				
b					82.9	5,060	31.9	0.349				
c					77.9	6,720	49.5	0.336				
d					74.7	8,185	77.0	0.287				
5a			3.65	738	115.6	4,950	4.5	1.027				
b					106.8	8,405	10.3	0.884				
c					101.7	11,450	16.3	0.847				
d					95.4	13,350	18.2	1.005				
6a				612	117.4	5,105	4.6	1.210				
b					110.5	8,995	10.8	1.030				
c					105.5	12,320	18.6	0.896				
d					101.1	14,990	24.6	0.892				

7a			4.50	492	127.5	6,020	3.7	1.256				Amplitude - Frequency Response Curves and Phase Angle-Frequency Curves
b					120.6	10,720	8.1	1.130				
c					106.8	12,630	12.0	1.150				
d					105.5	16,330	17.5	1.050				
8a				612	113.0	4,725	3.4	1.095				
b					105.5	8,200	6.8	1.090				
c					110.5	13,520	11.4	0.976				
d					105.5	16,330	16.3	0.903				
9a			5.17	369	106.1	4,165	2.4	1.925				
b					103.0	7,820	5.1	1.880				
c					99.2	10,890	7.7	1.820				
d					98.0	14,090	9.1	2.030				
10a				612	98.6	3,600	2.0	1.395				
b					97.3	6,975	4.3	1.292				
c					91.1	9,190	6.6	1.260				
d					95.4	13,350	9.7	1.140				
I-1a	Waterways Experiment Station[21]	Nonplastic uniform fine sand	2.58	1,225	100.5	3,740	8.6	0.649	1,044	250		
b					94.2	6,540	17.0	0.653				
c					94.2	9,825	25.2	0.661				
d					95.4	13,350	31.4	0.704				
2a			3.65	738	100.5	3,740	6.2	0.745				
b					95.4	6,705	12.2	0.754				
c					94.8	9,945	17.6	0.783				
d					94.2	13,020	22.8	0.803				
3a				612	99.2	3,645	9.2	0.610				
b					96.7	6,890	17.4	0.638				
c					95.4	10,070	24.0	0.693				
d					94.2	13,020	27.2	0.813				
4a				738	105.5	4,120	5.6	0.826				
b					101.7	7,625	10.3	0.893				
c					100.5	11,180	15.0	0.919				
d					98.6	14,260	20.8	0.880				
5a				612	108.0	4,320	9.9	0.564				
b					104.2	8,005	15.4	0.722				
c					102.4	11,610	19.2	0.868				
d					101.1	14,990	21.0	1.052				

TABLE I—*Continued*

1	2	3	4	5	6	7	8	9	10		11	12
No.	Reference	Soil	Radius of Foundation	Average Static Contact Pressure	Angular Resonance Frequency	Exciting Force Amplitude at Resonance	Displacement Amplitude at Resonance	Loss Coefficient of Soil-Foundation System at Resonance	Compression Wave Velocity	Shear Wave Velocity	Coefficient of Subgrade Reaction	Type of Available Data
			r_0 [ft]	$\bar{p}$ [lb/ft²]	ω_0 [Rad/sec]	$F_0 = m_1 e_0 \omega_0^2$ [lb]	y_{0r} [in × 10^{-3}]	η_s [—]	v_c [ft/sec]	v_s [ft/sec]	k_s [lb/ft²/in]	
I- continued	Waterways Experiment station[21] continued.	Nonplastic uniform fine sand continued.										
6a			4.50	492	100.5	3,740	9.2	0.502				Amplitude-Frequency Response Curves and Phase Angle-Frequency Curves
b					95.4	6,705	15.6	0.590				
c					93.6	9,700	23.0	0.600				
d					92.3	12,500	24.6	0.744				
7a				612	98.6	3,600	5.6	0.666				
b					92.9	6,360	11.8	0.629				
c					90.4	9,045	17.4	0.638				
d					89.2	11,670	21.8	0.677				
8a			5.17	369	102.4	3,880	8.5	0.543				
b					99.2	7,250	14.4	0.639				
c					96.1	10,220	19.0	0.726				
d					94.8	13,180	23.2	0.778				
9a				612	100.5	3,740	9.35	0.641				
b					94.2	6,540	9.10	0.612				
c					92.3	9,430	13.5	0.616				
d					90.4	11,980	18.0	0.615				
J-1a	F. J. Converse[22]	Sandpit	0.654	578	141	300						
b					147	300						
c					147	300						
d					136	400						
e					141	400						
f					141	400						
g					131	500						
h					136	500						

5-11					139	500						
j					133	600						
k					125	600						
2a				837	139	300						
b					134	450						
c					128	600						
3a			0.800	274	141	450						
b					149	300						
c					140	450						
d					146	300						
e					138	450						
4				304	144	300						
5a				389	128	600						Frequency at Maximum Amplitude
b					144	300						
c					141	450						
d					133	600						
e					131	750						
6a				405	128	600						
b					134	750						
c					131	750						
7a				532	136	300						
b					141	300						
c					147	300						
d					141	300						
e					136	450						
f					128	450						
g					131	450						
h					136	450						
i					136	450						
j					128	600						
k					131	600						
l					133	600						
m					131	600						
n					128	750						
o					126	750						
p					123	750						
q					121	800						
r					121	800						
s					126	800						

TABLE I—*Continued*

1	2	3	4	5	6	7	8	9	10		11	12
No.	Reference	Soil	Radius of Foundation	Average Static Contact Pressure	Angular Resonance Frequency	Exciting Force Amplitude at Resonance	Displacement Amplitude at Resonance	Loss Coefficient of Soil-Foundation System at Resonance	Compression Wave Velocity	Shear Wave Velocity	Coefficient of Subgrade Reaction	Type of Available Data
			r_0 [ft]	$\bar{p}$ [lb/ft²]	ω_0 [Rad/sec]	$F_0 = m_1 e_0 \omega_0^2$ [lb]	y_{0r} [in $\times 10^{-3}$]	η_s [—]	v_c [ft/sec]	v_s [ft/sec]	k_s [lb/ft²/in]	
K-1	F. J. Converse[22]	Beach Sand	0.800	222	163	300						
2a				387	163	300						
b					141	600						Frequency at Maximum Amplitude
3			1.875	100	157	650						
L-1a	H. Lorenz[23]	Peat	0.925	1,230	63.3							
b					69.0							
2a			1.85	307	74.0							Resonance of Frequency
b					82.2							
M-1	H. Lorenz[23]	Medium Sand	0.925	1,150	95.4							
2			1.850	287	109.3							
N-1	H. Lorenz[23]	Clayey Sand	0.925	1,253	135.3							
2			1.850	314	143.0							
P-1a	H. Lorenz[23]	?	1.85	556			98					Resonance Frequency and Amplitude of Resonance
b					122	5,200	118	0.192				
c							83					
d					113	4,320	130	0.175				
e					113	4,320	118	0.193				
f					113	4,320	130	0.177				
g					122	5,200	130	0.175				
2a			0.925	556	132	962	42.7	0.308				Amplitude-Frequency Re-
					113	1,410	86.5	0.337				

TABLE II — COMPRESSION AND SHEAR WAVE VELOCITIES OF SOME SOILS (FROM D. D. BARKAN)

Soil	Compression wave velocity [ft/sec]	Shear wave velocity [ft/sec]
Moist clay	4920	500
Loess at natural moisture	2630	850
Dense sand and gravel	1575	820
Fine-grained sand	985	360
Medium-grained sand	1800	525
Medium-sized gravel	2460	590

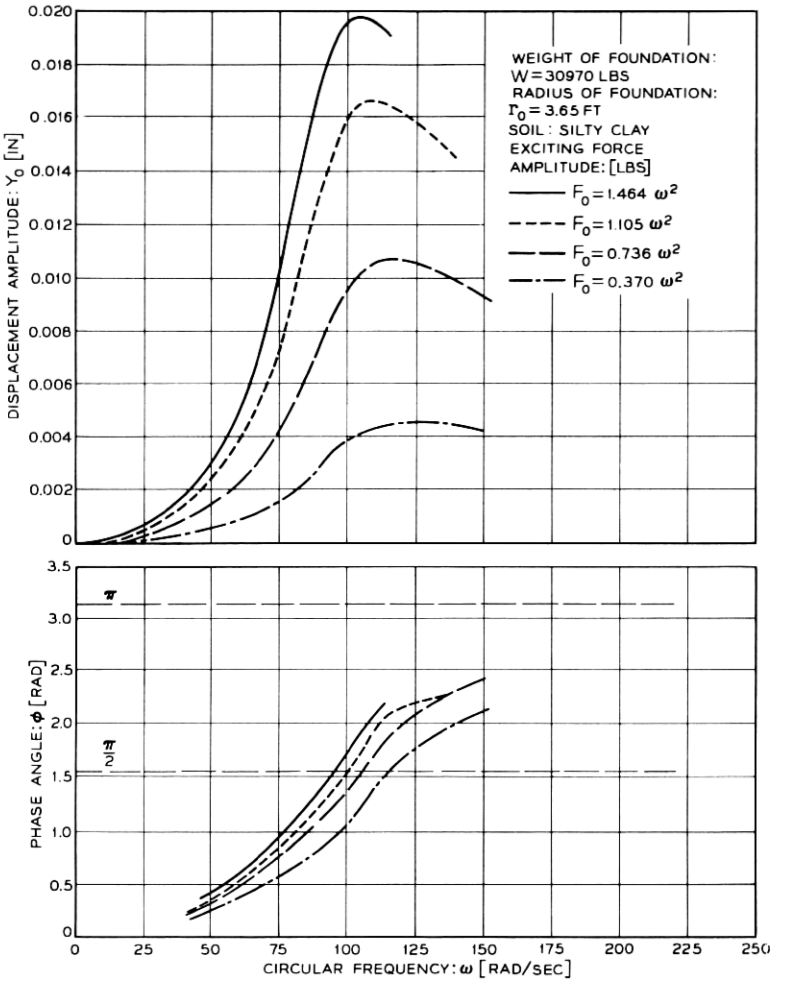

Fig. 4 — Typical amplitude-frequency response curve and phase angle-frequency curve of rigid circular foundation on silty clay.

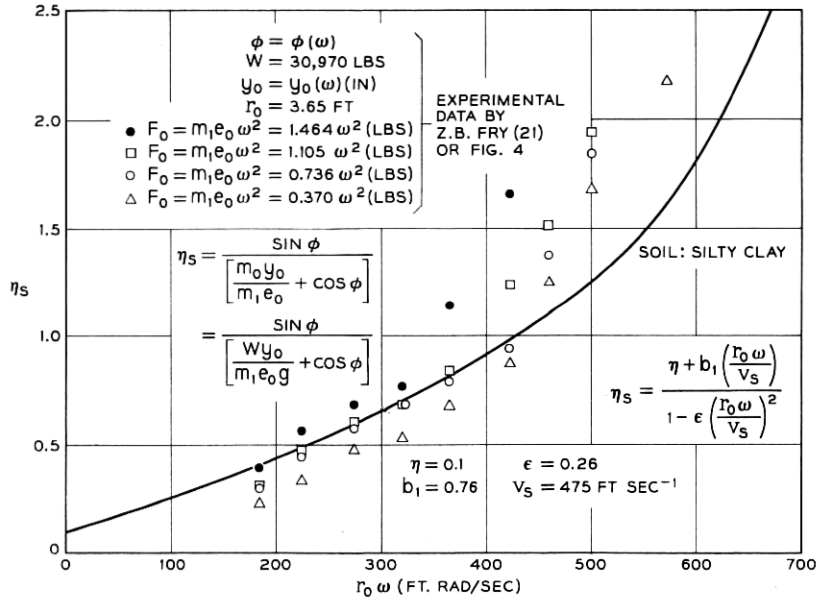

Fig. 5 — Loss coefficient of a vibrating circular foundation on silty clay.

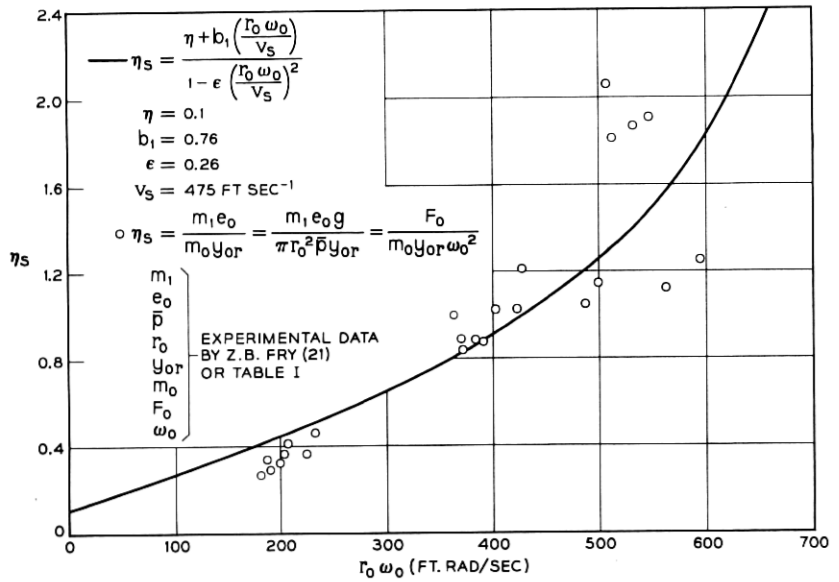

Fig. 6 — Loss coefficients at resonance of circular foundations on silty clay.

number of different shear wave velocities were substituted in (29) and the resulting curves are also shown in Fig. 7. Table II shows a value of the shear wave velocity of loess v_s = 850 ft/sec. The agreement of the predicted values of the loss coefficient and the experimentally determined values at resonance are again very good.

Z. B. Fry[21] reported also the results of vibration tests on sand. The resonance data, the radii, and the contact pressures are listed in Table I (I-1a to I-9d). A typical displacement amplitude-frequency response curve and the corresponding phase angle-frequency curve is shown in Fig. 8. The loss coefficients, η_s, were calculated by means of (47) and are shown in Fig. 9. No loss coefficient was predicted because the experimentally determined shear wave velocity decreased with an increase of the frequency. Fig. 10 shows the loss coefficients at resonance of foundations having different radii and contact pressures. The loss coefficient at resonance appears to be approximately constant. Fig. 11 shows the loss coefficients calculated by means of (47) for two foundations having different radii. The figure shows that for this sand, the loss coefficient is independent of the radius of the foundation. In order to obtain the constant loss coefficient at resonance shown in Fig. 10, the resonance frequency must be constant too. The resonance frequencies listed in Table I for this case are indeed almost constant.

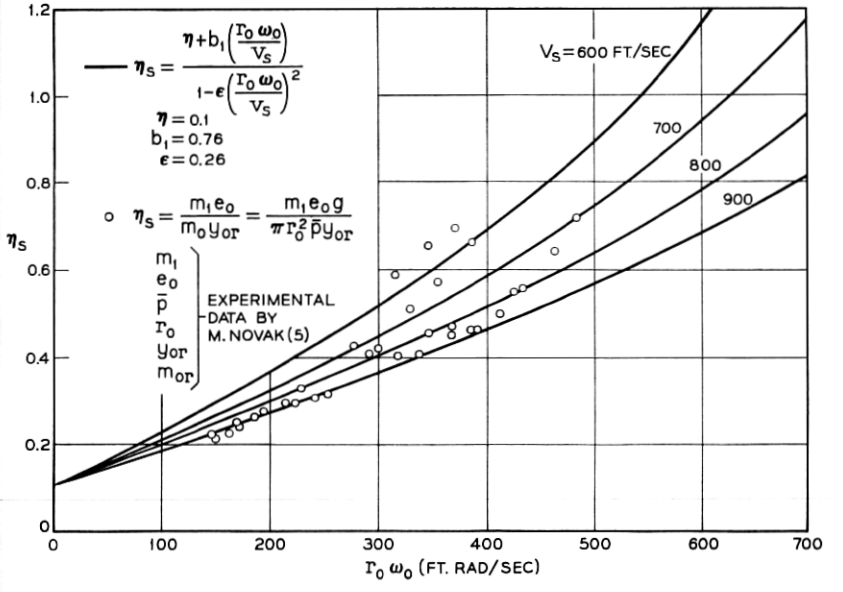

Fig. 7 — Loss coefficients at resonance of circular foundations on loess loam.

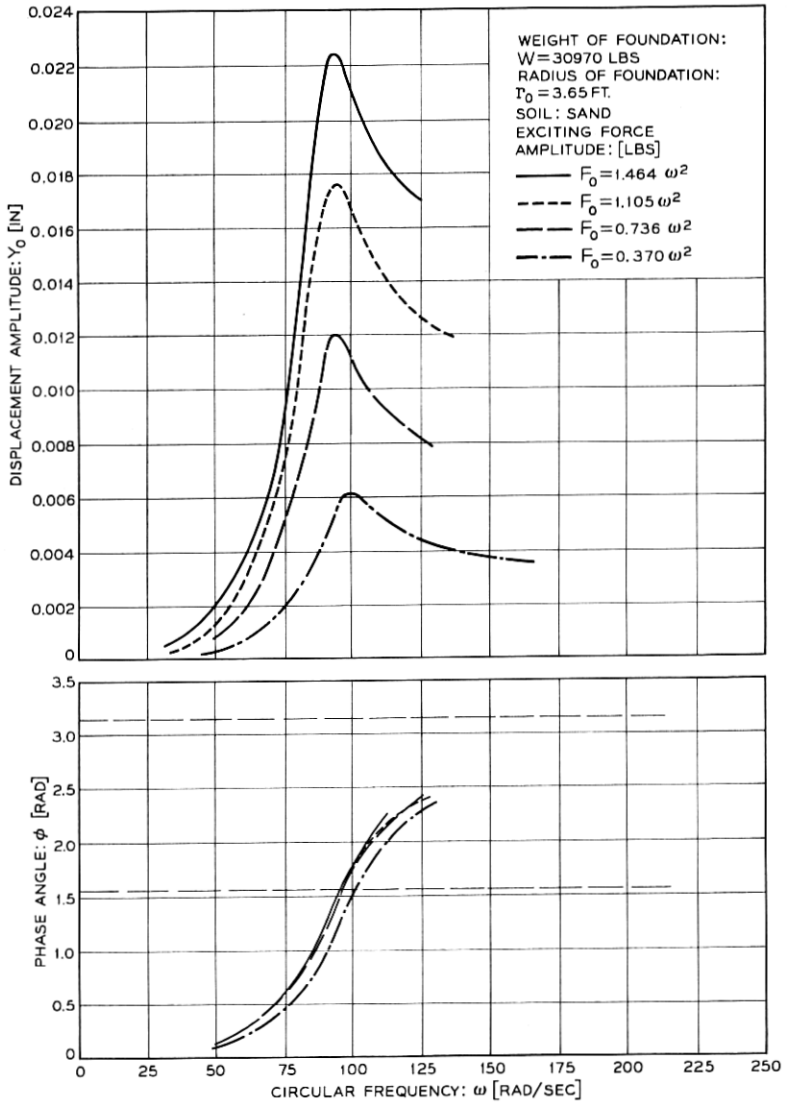

Fig. 8 — Typical amplitude-frequency response curve and phase angle-frequency curve of rigid circular foundation on sand.

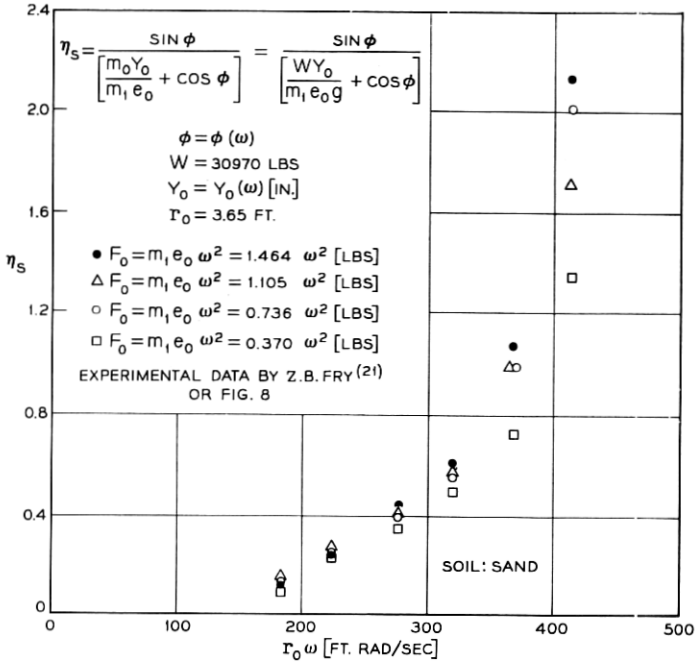

Fig. 9 — Loss coefficient of a vibrating circular foundation on sand.

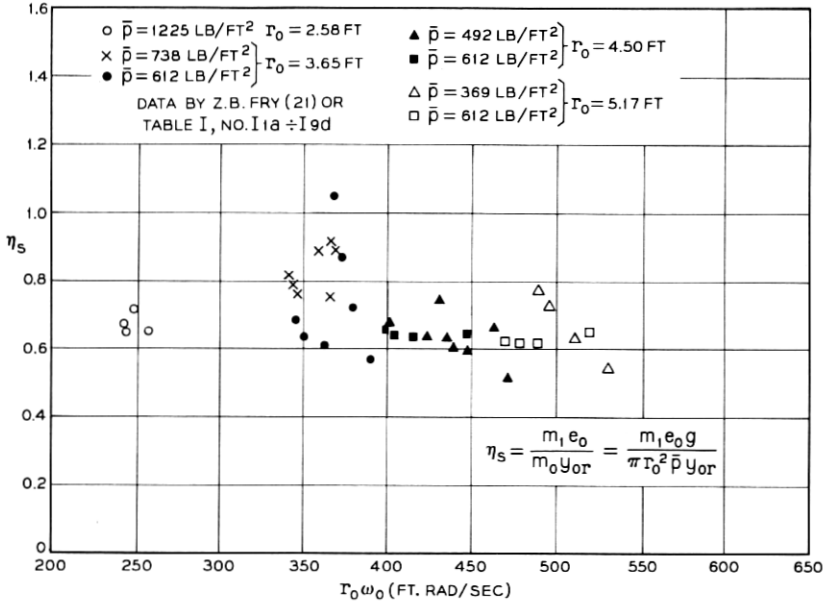

Fig. 10 — Loss coefficients at resonance of circular foundations on sand.

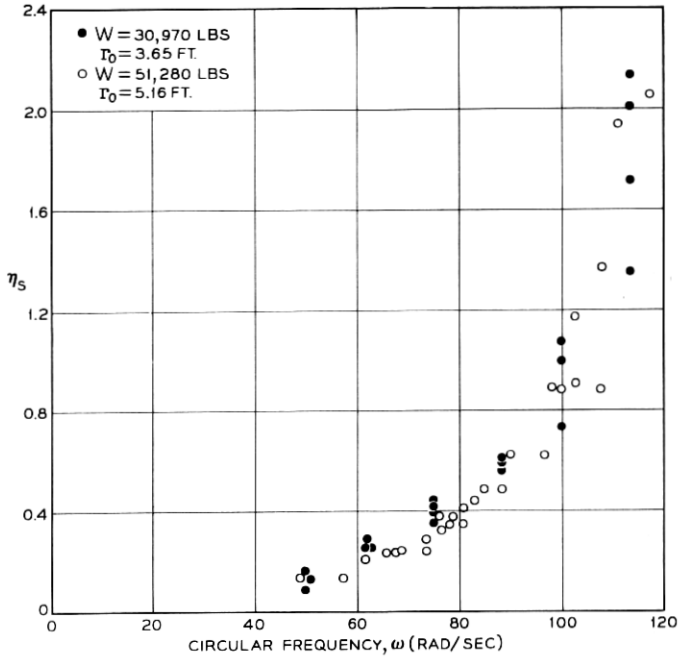

Fig. 11 — Loss coefficients of two different foundations on sand.

It may be concluded that the proposed mathematical model is capable of predicting the loss-coefficient, η_s, of a vibrating circular rigid foundation on a cohesive soil. For sand, however, this model is not applicable, and a different mechanism must be assumed in order to explain the independence of the loss coefficient from the magnitude of the radius of the foundation. The assumption of a dynamic arching effect causing the vibration of a large sand mass of a definite radius may provide an intuitive explanation.

The resonance frequency of the proposed mathematical model can be determined by means of (39). The resonance frequency depends on the coefficient of subgrade reaction, k_s, the static contact pressure, $\bar{p}$, the radius of the foundation, r_0, and the shear wave velocity, v_s. Equation (39) can frequently be replaced by (41), which neglects the inertia effects of the soil. It has been shown that these effects are relatively small for cohesive soils and foundations of small radii. The coefficient of subgrade reaction at the resonance frequency is generally slightly higher than the statically determined value. Hence, neglect of the effect

of the rate of loading in the numerator of (39) is often compensated by neglecting the inertia effects in the denominator.

The assumption, that the resonance frequency can be calculated by means of (41), is supported by the data obtained by D. D. Barkan[16] shown in Table I (B-1a to F-4). The calculated values of the resonance frequency, based on static load-deflection tests, agree well with the experimentally determined values. The error in percent is shown in Fig. 12 as a function of the radius of the foundation. The error does not exceed 20 percent. In general, the predicted values of the resonance frequency are higher than the experimentally determined ones. This was to be expected because the inertia effects of the soil are neglected in (41). Possible experimental errors may have caused the four predicted resonance frequencies shown in Fig. 12 which were lower than the experimentally determined values.

Unfortunately, to the best of the author's knowledge, only D. D. Barkan[16] determined the static coefficient of subgrade reaction in connection with vibration tests of circular foundations. However, the dynamic coefficient of subgrade reaction can be calculated by means of (45) provided the exciting force, displacement amplitude, and the phase angle are known experimentally determined functions of the frequency. The data shown in Fig. 4 were substituted in (45) and the dynamic coefficient of subgrade reaction was calculated for three different displacement amplitudes. The results are shown in Fig. 13. There is an expected scattering of the data. However, it may be concluded that the dynamic coefficient of subgrade reaction, $k_s\alpha$, decreases with an increase

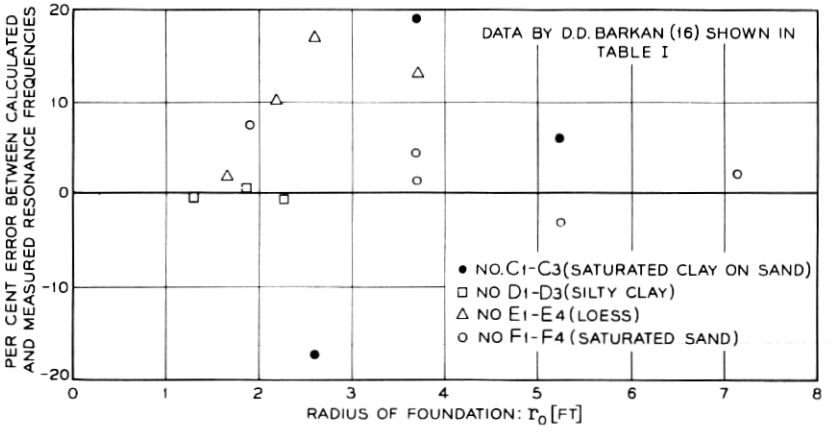

Fig. 12 — Error between calculated and measured resonance frequencies.

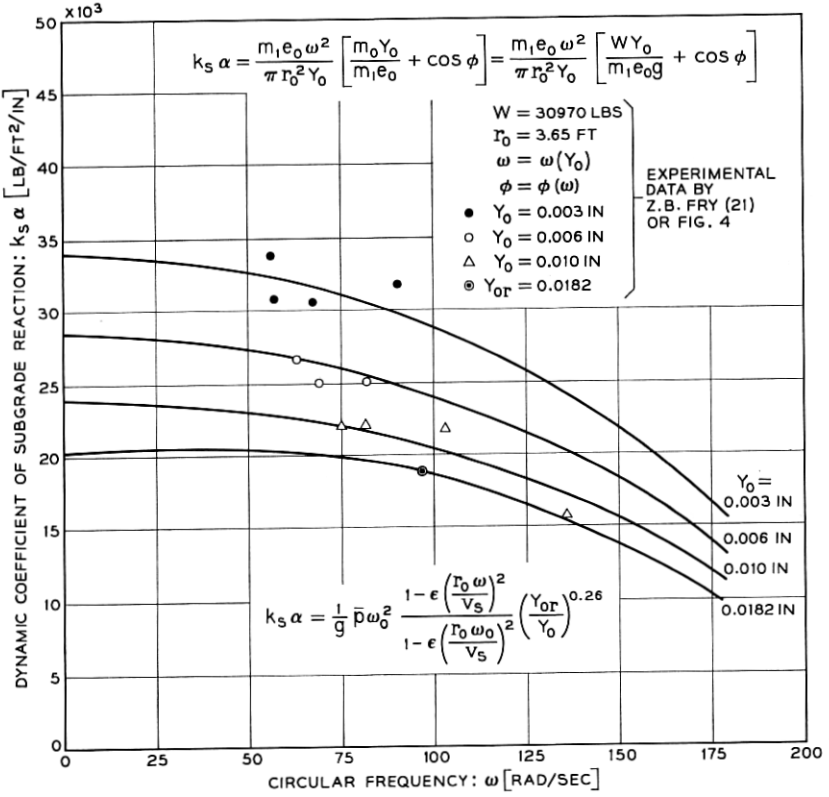

Fig. 13 — Dynamic coefficients of subgrade reaction as a function of the angular frequency for different displacement amplitudes on silty clay.

of the frequency, ω, at a constant displacement amplitude, y_0. Changes of the displacement amplitudes result, however, in significant changes of the coefficient of subgrade reaction.

Fig. 14 demonstrates the dependence of the dynamic coefficient of subgrade reaction on the displacement amplitude. The dynamic coefficient of subgrade reaction decreases with an increase of the displacement amplitude. For a constant frequency, the coefficient of subgrade reaction as a function of the displacement amplitude can be expressed with sufficient accuracy by the following empirical equation:

$$\frac{k_s}{k_s^*} = \left(\frac{y_0^*}{y_0}\right)^n \tag{48}$$

where

n = 0.26 = experimental constant,

k_s^* = coefficient of subgrade reaction at displacement amplitude y_0^*, and

y_0^* = displacement amplitude used as reference amplitude.

The maximum displacement amplitude at resonance, $y_{0r} = 0.0182$ in., is shown in Fig. 4 or in Table I, No. 5d and shall be used as reference amplitude ($y_0^* = y_{0r}$). Resonance occurred at $\omega_0^* = 95.4$ Rad. sec^{-1}. Solving (39) with respect to the coefficient of subgrade reaction, one obtains

$$k_s^* = \frac{\bar{p}^* \omega_0^{*2}}{g\left[1 - \varepsilon\left(\frac{r_0^* \omega_0^*}{v_s}\right)^2\right]} \tag{49}$$

provided the resonance frequency, ω_0^*, the shear wave velocity, v_s, the

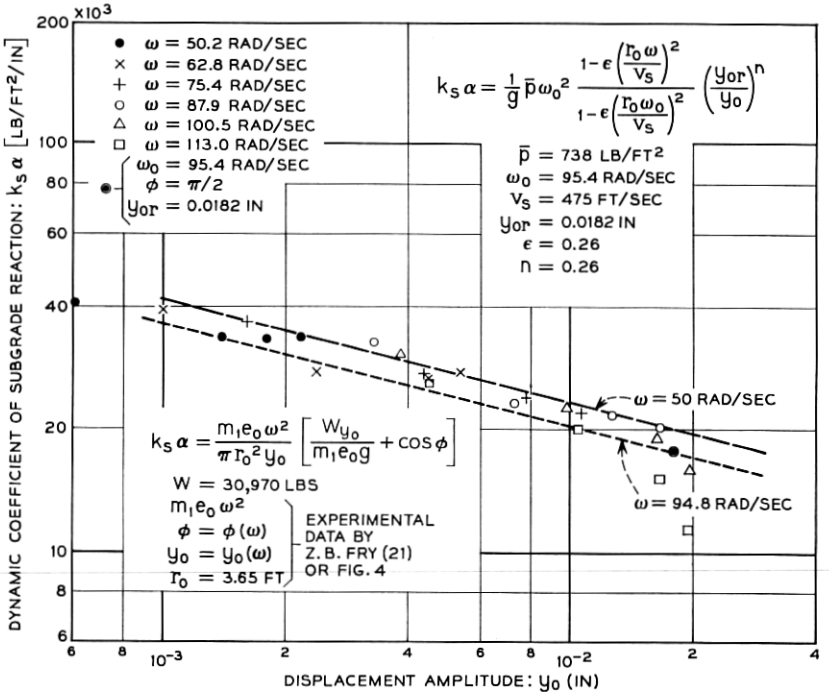

Fig. 14 — Dynamic coefficients of subgrade reaction as a function of the displacement amplitudes for different frequencies on silty clay.

average contact pressure, $\bar{p}^*$, and the radius, r_0^*, of the reference foundation are known quantities.

By means of (11), (48), and (49) the dynamic coefficient of subgrade reaction $k_s\alpha$ can be written as follows

$$k_s\alpha = \frac{\bar{p}^*\omega_0^{*2}}{g} \frac{\left[1 - \varepsilon\left(\frac{r_0^*\omega}{v_s}\right)^2\right]}{\left[1 - \varepsilon\left(\frac{r_0^*\omega_0^*}{v_s}\right)^2\right]} \left(\frac{y_0^*}{y_0}\right)^n. \tag{50}$$

Equation (50) is plotted in Fig. 13 for four values of the displacement amplitude, y_0, and in Fig. 14 for two values of the angular frequency, ω. A comparison of the data obtained by means of (45) with the plot of (50) shows that the results are compatible; however, the scattering of the experimental data prevents a direct verification of (50).

So far, the radius of the foundation, r_0, and the subsoil were assumed to remain constant. Now, however, the effect of a change of the radius and the contact pressure on the natural frequency of rigid circular foundations shall be considered. From (39) follows

$$\frac{\omega_0}{\omega_0^*} = \sqrt{\left(\frac{k_s}{k_s^*}\right)\left(\frac{\bar{p}^*}{\bar{p}}\right)\left[\frac{1 + \varepsilon\left(\frac{r_0^*}{v_s}\right)^2 \frac{k_s^* g}{\bar{p}^*}}{1 + \varepsilon\left(\frac{r_0^*}{v_s}\right)^2 \frac{k_s^* g}{\bar{p}^*}\left(\frac{r_0}{r_0^*}\right)^2\left(\frac{k_s}{k_s^*}\right)\left(\frac{\bar{p}^*}{\bar{p}}\right)}\right]}. \tag{51}$$

The asterisk indicates known quantities used for a reference foundation.

The coefficient of subgrade reaction is, as mentioned before, a function of the displacement amplitude, the radius of the foundation, the contact pressure, and the rate of loading. The author[17] proposed the following expression for the coefficient of subgrade reaction subjected to fluctuating loads

$$\frac{k_s}{k_s^*} = \left(\frac{y_0^*}{y_0}\right)^n \left[(1 - c^*)\left(\frac{r_0^*}{r_0}\right)^{(1-r)} + c^*\left(\frac{\bar{p}}{\bar{p}^*}\right)^p\right] \tag{52}$$

where n, r, c^*, and p are experimentally determined constants. If these constants are assumed to be zero, then (52) is proportional to (34) which is valid for the case of the elastic half-space, n indicates the amplitude dependent nonlinearity of the coefficient of subgrade reaction. An increase of the stiffness of the soil with depth is considered by the term $(r_0^*/r_0)^{(1-r)}$, and the effect of the contact pressure is indicated by $(\bar{p}/\bar{p}^*)^p$. It shall be assumed that the coefficients of subgrade reaction for fluc-

tuating loads were determined at a frequency in the range of the resonance frequencies of the vibrating foundations. Hence, no provision is made in (52) for the effect of the rate of loading. Substituting (52) in (51) one obtains

$$\frac{\omega_0}{\omega_0^*} = \left(\frac{y_{0r}^*}{y_{0r}}\right)^{n/2} \left(\frac{\bar{p}^*}{\bar{p}}\right)^{\frac{1}{2}} \left(\frac{r_0^*}{r_0}\right)^{\frac{1}{2}(1-r)} \left[1 - c^* + c^* \left(\frac{\bar{p}}{\bar{p}^*}\right)^p \left(\frac{r_0}{r_0^*}\right)^{(1-r)}\right]^{\frac{1}{2}}$$

$$\times \left[\frac{1 + \varepsilon \left(\frac{r_0^*}{v_s}\right)^2 \frac{k_s^* g}{\bar{p}^*}}{1 + \varepsilon \left(\frac{r_0^*}{v_s}\right)^2 \frac{k_s^* g}{\bar{p}^*} \left(\frac{y_{0r}^*}{y_{0r}}\right)^n \left(\frac{r_0}{r_0^*}\right)^{1+r} \left(\frac{\bar{p}^*}{\bar{p}}\right) \cdot \left[1 - c^* + c^* \left(\frac{\bar{p}}{\bar{p}^*}\right) \left(\frac{r_0}{r_0^*}\right)^{(1-r)}\right]}\right]^{\frac{1}{2}}. \quad (53)$$

Fig. 15 shows the angular resonance frequencies of the rigid circular foundations reported by Z. B. Fry[21] for silty clay as a function of the

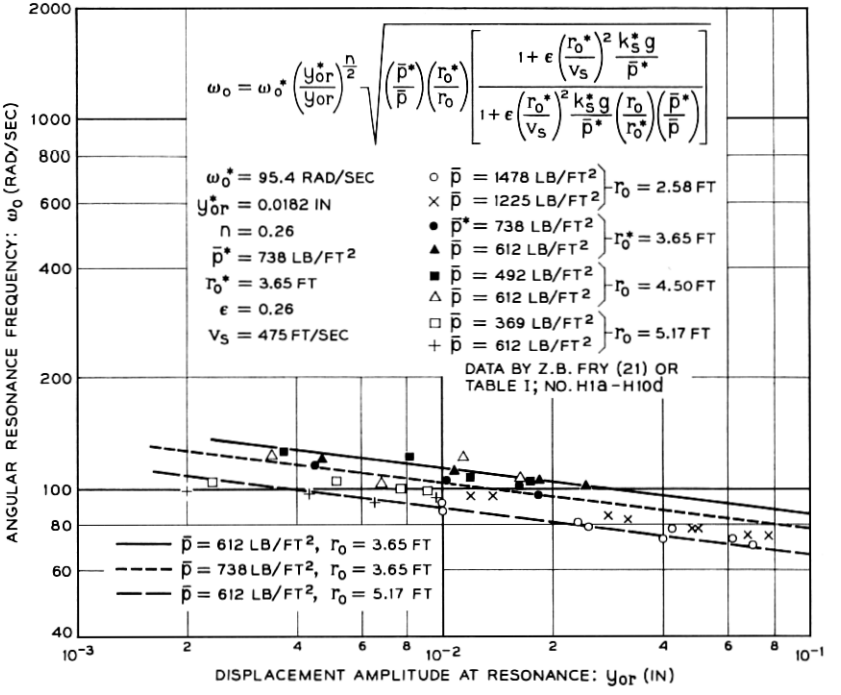

Fig. 15 — Resonance frequencies of rigid circular foundations on silty clay.

displacement amplitude at resonance. These data are listed in Table I, No. H-1a to H-10d. Z. B. Fry[21] reports furthermore, that the shear modulus determined by seismic methods does not change significantly with depth below the surface for this silty clay. Hence, it may be assumed that the constant, r, in (52) and (53) becomes approximately zero. Furthermore, it can be assumed that the effect of the static contact pressure can be neglected, since the overburden does not increase the shear modulus significantly. Hence, c^* is assumed to be small compared to unity. With these assumptions, (53) simplifies to

$$\frac{\omega_0}{\omega_0{}^*} = \left(\frac{y_{0r}{}^*}{y_{0r}}\right)^{n/2} \left(\frac{\bar{p}^*}{\bar{p}}\right)^{\frac{1}{2}} \left(\frac{r_0{}^*}{r_0}\right)^{\frac{1}{2}} \cdot \left[\frac{1 + \varepsilon\left(\frac{r_0{}^*}{v_s}\right)^2 \frac{k_s{}^* g}{\bar{p}^*}}{1 + \varepsilon\left(\frac{r_0{}^*}{v_s}\right)^2 \frac{k_s{}^* g}{\bar{p}^*}\left(\frac{r_c}{r_0{}^*}\right)\left(\frac{\bar{p}^*}{\bar{p}}\right)\left(\frac{y_{0r}{}^*}{y_{0r}}\right)^n}\right]^{\frac{1}{2}} \tag{54}$$

where

$\omega_0{}^*$ = 95.4 Rad/sec = angular resonance frequency of reference foundation for maximum exciting force listed in Table I, No. H-5d,

$y_{0r}{}^*$ = 0.0182 in. = amplitude at resonance of reference foundation,

$r_0{}^*$ = 3.65 ft = radius of reference foundation,

$\bar{p}^*$ = 738 lb/ft^2 = average static contact pressure of reference foundation,

ε = 0.26,

g = 386 in./sec^2 = acceleration of gravity,

v_s = 475 ft/sec = shear wave velocity,

n = 0.26 = experimental constant determined from Fig. 14, and

$k_s{}^*$ = coefficient of subgrade reaction for reference foundation calculated by (49).

For the contact pressure $\bar{p} = \bar{p}^* = 738$ lbs/ft^2 and the radius $r_0 = r_0{}^* = 3.65$ ft, the angular resonance frequency of the reference foundation is obtained and shown in Fig. 15 as a function of the displacement amplitude at resonance, y_{0r}. This curve fits the corresponding experimental data very well, which was to be expected from the results shown in Fig. 14. For a contact pressure $\bar{p} = 612$ lbs/ft^2 and a radius $r_0 = 3.65$ ft the maximum values of the angular resonance frequencies of the here considered foundations are obtained. For $\bar{p} = 612$ lbs/ft^2 and $r_0 =$

5.17 ft follow the minimum values. They are also shown in Fig. 15 as functions of the displacement amplitude at resonance. The experimental data and the curves computed by means of (54) show good agreement. It should be realized that the changes of the radii and the contact pressures were relatively small and their effects on the resonance frequency appear to be in the same order of magnitude as the possible experimental errors of measuring the resonance frequency. However, the dependence of the resonance frequency on the displacement amplitude is clearly demonstrated.

The resonance frequencies obtained by M. Novák on a loess loam are listed in Table I, No. A-1a to A-10c. They are shown in Fig. 16 as a function of the displacement amplitude at resonance. Again it is apparent, that the resonance frequency decreases with an increase of the displacement amplitude; however, not as rapidly as in Fig. 15. Unfortunately, no detailed description of the soil properties is available; however, it has been shown in Fig. 7 that an assumed shear wave velocity $v_s = 800$ ft/sec allowed the prediction of the loss coefficient with good accuracy. Hence, the term $\varepsilon(r_0/v_s)^2$ becomes small compared to

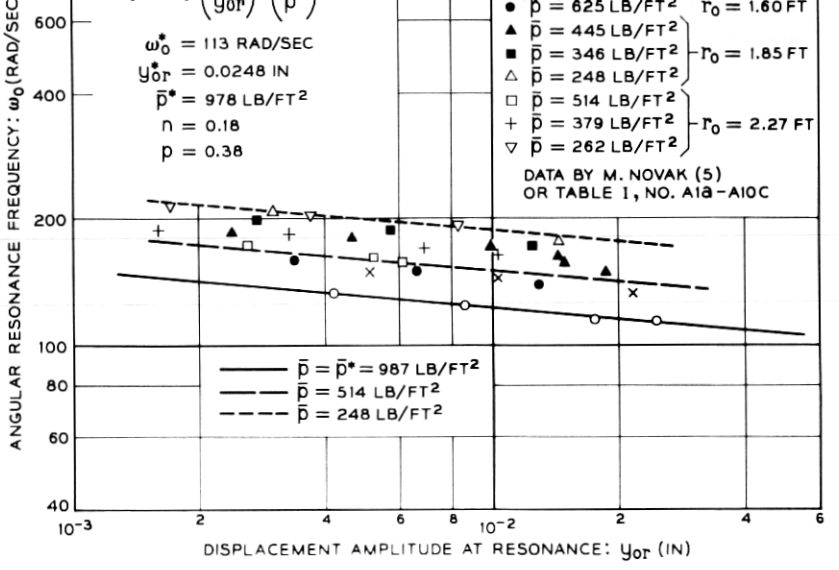

Fig. 16 — Resonance frequencies of rigid circular foundations on loess loam.

one and can be neglected in (53). Equation (53) can then be written

$$\frac{\omega_0}{\omega_0{}^*} = \left(\frac{y_{0r}{}^*}{y_{0r}}\right)^{n/2} \left(\frac{\bar{p}^*}{\bar{p}}\right)^{\frac{1}{2}} \left[(1 - c^*)\left(\frac{r_0{}^*}{r_0}\right)^{(1-r)} + c^*\left(\frac{\bar{p}}{\bar{p}^*}\right)^{p}\right]^{\frac{1}{2}}. \quad (55)$$

For each set of data shown in Fig. 16 follows $n = 0.18$. Assuming $c^* \approx 1$ and $p = 0.38$, (55) becomes

$$\frac{\omega_0}{\omega_0{}^*} = \left(\frac{y_{0r}{}^*}{y_{0r}}\right)^{n/2} \left(\frac{\bar{p}^*}{\bar{p}}\right)^{\frac{1}{2}(1-p)} = \left(\frac{y_{0r}{}^*}{y_{0r}}\right)^{0.09} \left(\frac{\bar{p}^*}{\bar{p}}\right)^{0.31}. \quad (56)$$

Equation (56) shows the effect of a change of the displacement amplitude and of the contact pressure on the resonance frequcncy for the data shown in Fig. 15. The agreement between the resonance frequencies calculated by use of (56) and the experimental data is excellent.

The assumption of $c^* \approx 1$ in (56) results in a resonance frequency which is not affected by a change of the radius of the foundation. Since this is possible only if the overburden increases the stiffness of the soil, the stiffness of the soil must also be affected by the magnitude of the contact pressure $\bar{p}$. Hence, an experimental constant $p = 0.38$, which indicates the effect of the contact pressure on the stiffness of the soil, is reasonable.

The effect of a change of the radius of the foundation on the resonance frequency shall now be discussed. The resonance frequencies of the foundations described by (54) decrease with an increase of the radius. The decrease of the resonance frequency is approximately proportional to the square root of the radius. A similar relationship between the resonance frequency and the radius of the foundation was established by G. P. Tschebotarioff[24] who evaluated the performance records of a limited number of existing engine foundations. However, foundations, which are described by (56), are independent of the radius. H. Lorenz[23] reported an increase of the resonance frequency due to an increase of the radius. This apparent contradiction is readily explained by the proven nonlinearity of the coefficient of subgrade reaction. The exciting force in all test results here reported was produced by eccentrically rotating weights. Therefore, the ratio of the displacement amplitudes at resonance becomes, by means of (43),

$$\frac{y_{0r}{}^*}{y_{0r}} = \left(\frac{m_1{}^* e_0{}^*}{m_1 e_0}\right)\left(\frac{\omega_0{}^*}{\omega_0}\right)^2 \left(\frac{k_s}{k_s{}^*}\right)\left(\frac{r_0}{r_0{}^*}\right)^2 \cdot \left[\frac{\eta + b_1 \dfrac{r_0{}^*\omega_0{}^*}{v_s}\left(\dfrac{r_0}{r_0{}^*}\right)\left(\dfrac{\omega_0}{\omega_0{}^*}\right)}{\eta + b_1 \dfrac{r_0{}^*\omega_0{}^*}{v_s}}\right]. \quad (57)$$

Substituting (57) in (52) and solving for the ratio of the displacement amplitudes at resonance and substituting this ratio in (53) the following expression for the resonance frequency is obtained:

$$\frac{\omega_0}{\omega_0^*} = \left(\frac{m_1^* e_0^*}{m_1 e_0}\right)^{n/2} \left(\frac{r_0^*}{r_0}\right)^{\frac{1}{2}(1-r-2n)} \left(\frac{\bar{p}^*}{\bar{p}}\right)^{\frac{1}{2}(1-n)} \cdot \left[1 - c^* + c^* \left(\frac{r_0}{r_0^*}\right)^{(1-r)} \left(\frac{\bar{p}}{\bar{p}^*}\right)^{p}\right]^{\frac{1}{2}} c_1^{n/2} c_2^{\frac{1}{2}(1-n)} \tag{58}$$

where

$$c_1 = \frac{\eta + b_1 \dfrac{r_0^* \omega_0^*}{v_s} \left(\dfrac{y_{0r}^*}{y_{0r}}\right)^{n/2} \left(\dfrac{r_0}{r_0^*}\right)^{\frac{1}{2}(1+r)} \left(\dfrac{\bar{p}^*}{\bar{p}}\right)^{\frac{1}{2}} c_2^{\frac{1}{2}} \cdot \left[1 - c^* + c^* \left(\dfrac{r_0}{r_0^*}\right)^{(1-r)} \left(\dfrac{\bar{p}}{\bar{p}^*}\right)^{p}\right]^{\frac{1}{2}}}{\eta + b_1 \dfrac{r_0^* \omega_0^*}{v_s}}$$

$$c_2 = \frac{1 + \varepsilon \left(\dfrac{r_0^*}{v_s}\right)^2 \dfrac{k_s^* g}{\bar{p}^*}}{1 + \varepsilon \left(\dfrac{r_0^*}{v_s}\right)^2 \dfrac{k_s^* g}{\bar{p}^*} \left(\dfrac{y_{0r}^*}{y_{0r}}\right)^n \left(\dfrac{r_0}{r_0^*}\right)^{1+r} \left(\dfrac{\bar{p}^*}{\bar{p}}\right) \cdot \left[1 - c^* + c^* \left(\dfrac{r_0}{r_0^*}\right)^{(1-r)} \left(\dfrac{\bar{p}}{\bar{p}^*}\right)^{p}\right]}.$$

Since $n \ll 1$, $(y_{0r}^*/y_{0r})^n$, and $c_1^{n/2}$ are approximately equal to one. For $c^* = 0$, (58) becomes

$$\frac{\omega_0}{\omega_0^*} = \left(\frac{m_1^* e_0^*}{m_1 e_0}\right)^{n/2} \left(\frac{r_0^*}{r_0}\right)^{\frac{1}{2}(1-r-2n)} \left(\frac{\bar{p}^*}{\bar{p}}\right)^{\frac{1}{2}(1-n)} \cdot \left[\frac{1 + \varepsilon \left(\dfrac{r_0^*}{v_s}\right) \dfrac{k_s^* g}{\bar{p}^*}}{1 + \varepsilon \left(\dfrac{r_0^*}{v_s}\right)^2 \dfrac{k_s^* g}{\bar{p}^*} \left(\dfrac{r_0}{r_0^*}\right)^{(1+r)} \left(\dfrac{\bar{p}^*}{\bar{p}}\right)}\right]^{\frac{1}{2}(1-n)}. \tag{59}$$

For $c^* = 1$, it follows

$$\frac{\omega_0}{\omega_0^*} = \left(\frac{m_1^* e_0^*}{m_1 e_0}\right)^{n/2} \left(\frac{r_0}{r_0^*}\right)^{n} \left(\frac{\bar{p}^*}{\bar{p}}\right)^{\frac{1}{2}(1-n-p)} \cdot \left[\frac{1 + \varepsilon \left(\dfrac{r_0^*}{v_s}\right)^2 \dfrac{k_s^* g}{\bar{p}^*}}{1 + \varepsilon \left(\dfrac{r_0^*}{v_s}\right) \dfrac{k_s^* g}{\bar{p}^*} \left(\dfrac{r_0}{r_0^*}\right)^{2} \left(\dfrac{\bar{p}^*}{\bar{p}}\right)^{(1-p)}}\right]^{\frac{1}{2}(1-n)}. \tag{60}$$

The resonance frequencies of vibrating foundations which are expressed in terms of (59) are affected by the nonlinearity of the coefficient of subgrade reaction. For relatively small foundation radii and relatively large nonlinearities expressed by the experimental constant, n, an increase of the radius may result in an increase of the resonance frequency. For large foundation radii and small nonlinearities, however, the frequency should decrease for an increase of the radius. Resonance frequencies expressed in terms of (60) should show an increase of the resonance frequency with an increase of the radius.

Equations (59) and (60) show also the effect of the contact pressure, $\bar{p}$, on the resonance frequency. Generally, the resonance frequency decreases for an increase of the contact pressure, however, at a rate less than expected from purely elastic considerations. The nonlinearities expressed by the experimental constant, n, in (59) and (60) reduces the effect of the contact pressure which is proportional to the mass of the foundation. The stiffening effect of the contact pressure is expressed by the experimental constant, p. The value of $p = 0.38$ was used to express the data shown in Fig. 16. In the plate bearing tests conducted by the author and S. R. White[18], a value of $p = 1.859$ was obtained. For such a soil, an increase of the resonance frequency with an increase of the static contact pressure should be expected. In other words, the increase of the mass of the vibrating system is more than compensated by the resulting increase of the stiffness.

It may be stated, that the proposed mathematical model is not only not contradicted by the available experimental data obtained on silty clay and loess loam, but that there is a satisfactory amount of evidence supporting this theory.

Equation (45) was also used to calculate the dynamic coefficient of subgrade reaction for sand. The amplitude-frequency response curve and the phase angle-frequency curve shown in Fig. 8 were used for the calculation. The dynamic coefficient of subgrade reaction, $k_s\alpha$, divided by the contact pressure, $\bar{p}$, and multiplied by the acceleration of gravity is shown in Fig. 17 as a function of the frequency. The data show a strong dependence on the frequency. The dynamic coefficient of subgrade reaction decreases rapidly if the frequency is increased. This phenomenon was to be expected, because the loss coefficient increased rapidly with an increase of the frequency as shown in Figs. 9 and 11. However, the shape of the dynamic coefficient of subgrade reaction-frequency curve does not agree with the shape of the function α shown in Fig. 2. Hence, the proposed mathematical model of the vibrating rigid circular foundation is not applicable to foundation-sand systems. The dynamic coefficient

of subgrade reaction was also determined for two additional foundations. The amplitude-frequency response curves and the phase angle-frequency curves of these foundations were also provided by Z. B. Fry[21] of the U.S. Waterways Experiment Station. The dynamic coefficients of subgrade reaction divided by the contact pressure and multiplied by the acceleration of gravity for these additional foundations are also shown in Fig. 17. There appears to be a difference of the dynamic coefficient of subgrade reaction divided by the contact pressure for low frequencies. For higher frequencies, however, the data are practically identical. This implies a coefficient of subgrade reaction proportional to the contact pressure and independent of the radius of the foundation. The intersection of the ω^2-curve with the data indicates the resonance frequency. For the three sets of data shown in Fig. 17, the resonance frequency appears to be constant. In order to verify this assumption, all the resonance frequencies reported by Z. B. Fry[21] are shown in Fig. 18 as a func-

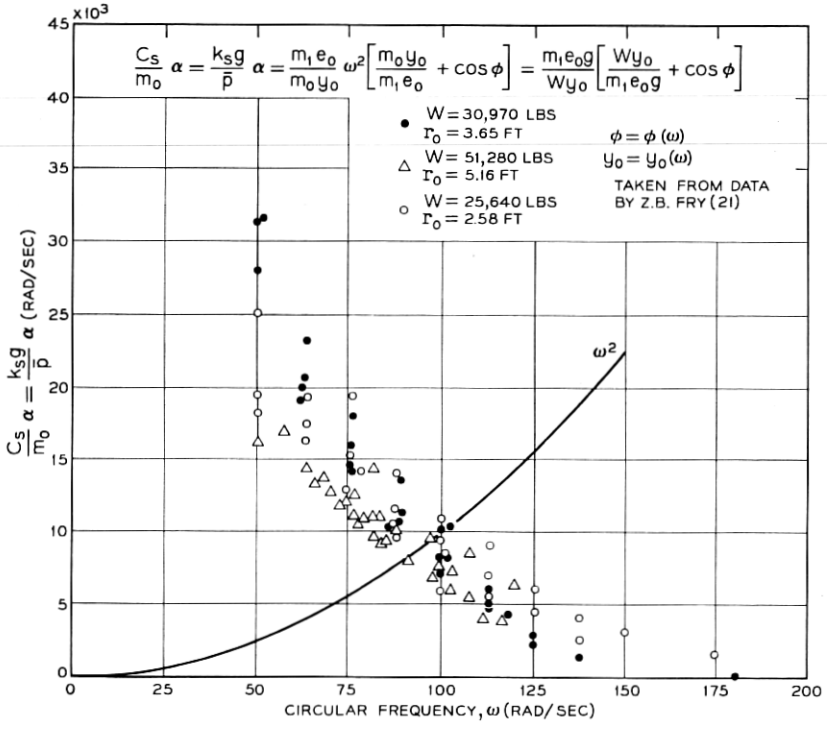

Fig. 17 — Dynamic coefficients of subgrade reaction as a function of the frequency on sand for three different foundations.

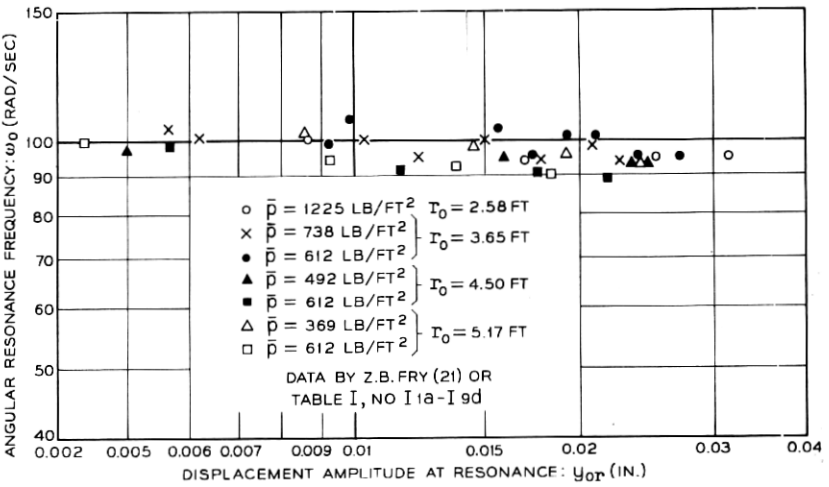

Fig. 18 — Resonance frequencies of rigid circular foundations on sand.

tion of the displacement amplitudes. For all practical purposes, the resonance frequencies for these circular foundations on sand are constant, independent of displacement amplitude, radius, and contact pressure. The data by F. J. Converse[22] listed in Table I, No. J-1a to J-7s, show a dependence on the applied force amplitude but appear to be relatively independent of the contact pressure and the radius. A mechanism describing the vibrations of circular foundations on sand must be different from the here proposed mathematical model. Arching of sand has probably a significant effect on the vibrations of foundation-sand systems. For engineering purposes, it appears to be sufficient to determine the resonance frequency and the loss coefficient with a small vibrator and to assume an identical resonance frequency and loss coefficient of the planned foundation. The suggestion by G. P. Tschebotarioff[25] of providing cavities near the four corners of machine foundation blocks which could be filled, or emptied, to change the weight of the block by 15 to 20 percent would have no or only an insignificant effect on the resonance frequency and the loss coefficient of foundations on sand.

The effective mass of a vibrating rigid circular plate on an elastic isotropic homogeneous half-space is determined by (15). The mass of the half-space vibrating in phase with the plate becomes

$$m_s = \varepsilon C_s \left(\frac{r_0}{v_s}\right)^2 \tag{61}$$

where

m_s = mass of half-space vibrating in phase with plate.

The ratio of the soil mass to the mass of the plate becomes, by means of (61), (33), and (35),

$$\frac{m_s}{m_0} = \varepsilon \frac{k_s g}{\bar{p}} \left(\frac{r_0}{v_s}\right)^2. \tag{62}$$

Substitution of (49) in (62) gives

$$\frac{m_s}{m_0} = \frac{\varepsilon \left(\frac{r_0\omega_0}{v_s}\right)^2}{1 - \varepsilon \left(\frac{r_0\omega_0}{v_s}\right)^2}. \tag{63}$$

The validity of (63) is limited to values of $r_0\omega_0/v_s \leqq 1.5$. For this value, the ratio of the participating soil mass to the mass of the vibrating plate becomes 1.41. For most vibrating foundations listed in Table I, this ratio becomes considerably smaller and the participating soil mass, m_s, becomes insignificantly small for small foundations. This conclusion is apparently contradicted by the theoretical and experimental investigations of W. Heukelom.[13,14] However, it is readily shown, that the amplitude dependent nonlinearity of the soil, which he recognized but neglected, can account for this apparent contradiction. The dynamic stiffness can be calculated by means of (20) from experimentally determined displacement amplitudes and phase angles. The vibration data obtained by Z. B. Fry[21] shall be used again to calculate the dynamic stiffness. The displacement amplitude-frequency curve as well as some values of the dynamic stiffness, calculated by means of (20), are shown in Fig. 19. No provision was made to account for the nonlinearity of the load-deflection characteristic of the soil. W. Heukelom[13,14] fitted to such experimental data the following function:

$$\begin{aligned} S &= S\,|_{\omega=0} - m_s\omega^2 && \text{for} \quad \omega \leqq \omega_0 \\ &= S\,|_{\omega=0} - m_s \left(\frac{\omega_0}{\omega}\right)^3 \omega^2 && \text{for} \quad \omega_0 \leqq \omega. \end{aligned}$$

The constants $S\,|_{\omega=0}$ and m_s, representing the static stiffness and the participating soil mass, can be selected to fit the experimental data very well indeed. This equation would indicate a constant participating soil mass, m_s, for frequencies below the resonance frequency and a participating soil mass, $m_s(\omega_0/\omega)^3$, decreasing with an increase of the frequency for frequencies greater than the resonance frequency. The magnitude of

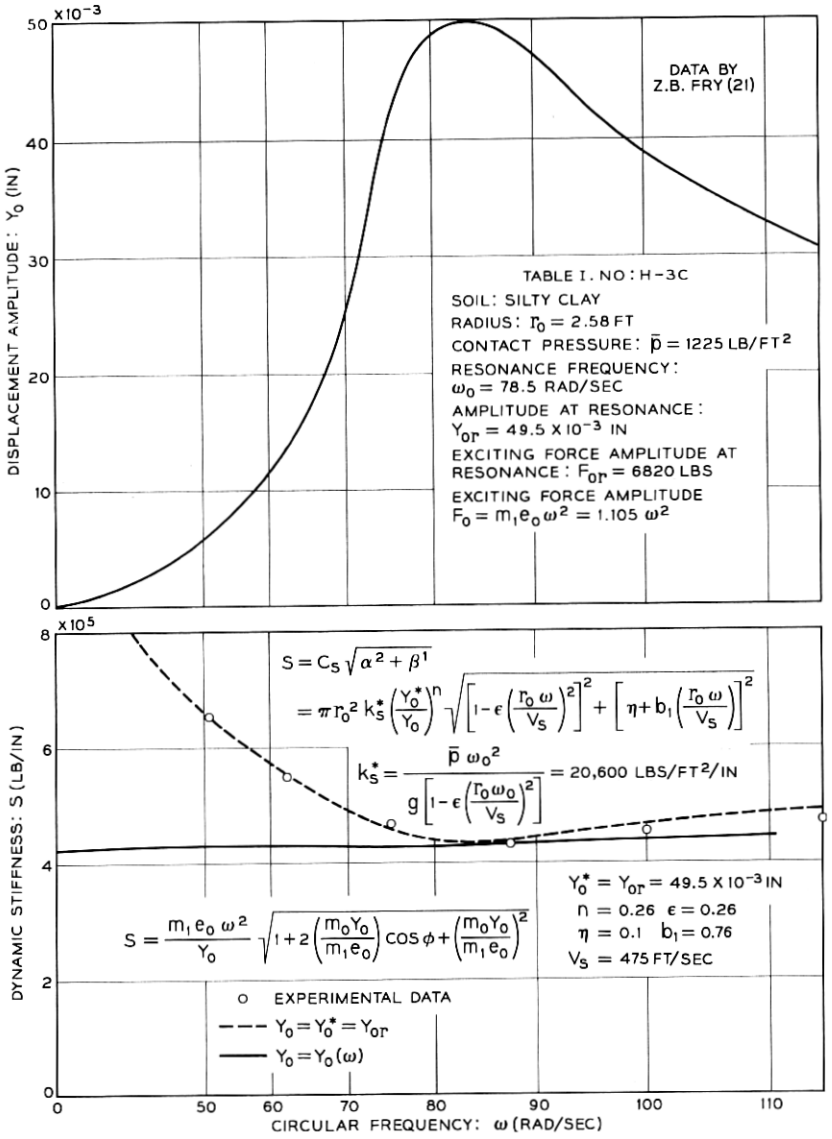

Fig. 19 — Effect of the displacement amplitude on the dynamic stiffness.

the participating soil mass becomes considerably larger than that obtained by (63).

The dynamic stiffness of the proposed mathematical model is obtained by substitution of (33), (28), and (11) in (21)

$$S = \pi r_0^2 k_s \sqrt{\left[1 - \varepsilon \left(\frac{r_0\omega}{v_s}\right)^2\right]^2 + \left[\eta + b_1 \left(\frac{r_0\omega}{v_s}\right)\right]^2} \tag{64}$$

and by substitution of (48) as

$$S = \pi r_0^2 k_s^* \left(\frac{y_0^*}{y_0}\right)^n \sqrt{\left[1 - \varepsilon \left(\frac{r_0\omega}{v_s}\right)^2\right]^2 + \left[\eta + b_1 \left(\frac{r_0\omega}{v_s}\right)\right]^2}. \tag{65}$$

where k_s^* is determined from (49). For the resonance frequency, $\pi r_0^2 k_s$ becomes 420,000 lbs/in. The displacement amplitude at resonance $y_{0r} = y_0^* = 0.0495$ in. and the experimental constant $n = 0.26$ are used for the calculations. The solid line in Fig. 19 indicates the dynamic stiffness for a constant displacement amplitude $y_0 = y_0^* = y_{0r}$. As is to be expected, this curve fits the data only at the resonance frequency. The dotted line, however, shows the corrections made to account for the amplitude dependence of the dynamic stiffness expressed by $(y_0^*/y_0)^n$. The displacement amplitude, y_0, at each frequency is taken from the displacement amplitude-frequency curve also shown in Fig. 19. The dotted curve fits the experimental data very well. It should be noted here that this curve was rationally developed and not obtained by direct fitting of data. It may be concluded that the reduction of the dynamic stiffness close to resonance is caused by the amplitude dependent nonlinearity of the load deflection characteristic of the soil-foundation system and not by a frequency dependent mass or a frequency dependent coefficient of subgrade reaction. Even a small nonlinearity will cause a significant change of the dynamic stiffness close to resonance due to the large amplitude changes occurring in this frequency range. Again, the proposed mathematical model is applicable only for cohesive soils and no attempt was made to calculate the dynamic stiffness of sand-foundation systems.

XI. SUMMARY AND CONCLUSIONS

The displacement amplitudes and the phase angles of vertically vibrating rigid circular foundations on soil have been expressed in terms of the average static contact pressure between the foundation and the subsoil, the coefficient of subgrade reaction for fluctuating loads, the magnitude and frequency of the exciting force, the radius of the founda-

tion, the loss coefficient of the soil, the shear wave velocity, and two theoretically derived constants accounting for the inertia effects of the soil. The nonlinear stress-deflection characteristic of the coefficient of subgrade reaction as well as the dependence of the coefficient of subgrade reaction on the radius of the foundation and the average contact pressure between the foundation and the subsoil have been considered. The derived mathematical model describes, as a limiting idealized case, the vibrations of rigid circular plates on an elastic isotropic homogeneous solid. Furthermore, it is capable of expressing the static load-deflection characteristics of rigid circular foundation on soil and, as a limiting case, on an elastic half-space.

Based on this mathematical model, the following behavior of a vibrating soil-foundation system should be expected:

(*i*) An increase of the exciting force amplitude results in a decrease of the resonance frequency of the vibrating foundation. This effect is caused by the nonlinearity of the coefficient of subgrade reaction.

(*ii*) An increase of the radius of the foundation when maintaining a constant contact pressure and exciting force can result in either an increase or a decrease of the resonance frequency of the vibrating soil-foundation system. For large foundations an increase of the radius will generally result in a decrease of the resonance frequency. For smaller foundations the nonlinearity of the coefficient of subgrade reaction and the increase of the stiffness of the soil with depth may cause an increase of the resonance frequency for an increase of the radius of the foundation. For small nonlinearities of the coefficient of subgrade reaction and small increases of the stiffness of the soil with depth, an increase of the radius of the foundation will cause a decrease of the resonance frequency.

(*iii*) An increase of the contact pressure will generally lower the resonance frequency, however, less than would be expected from purely elastic considerations. The nonlinearity of the coefficient of subgrade reaction and the increase of the coefficient of subgrade reaction with an increase of the applied static contact pressure explain this phenomenon. For some soils an increase of the contact pressure could possibly result in an increase of the resonance frequency if the coefficient of subgrade reaction increases very rapidly with an increase of the static contact pressure.

(*iv*) The loss coefficient, expressing the damping of the vibrating

system, increases with an increase of the radius of the foundation. The inertia effects of the soil or of an elastic half-space account for this behavior.

(*v*) The displacement amplitudes increase less than proportional to the amplitudes of the exciting force. Again, the nonlinearity of the coefficient of subgrade reaction explains this phenomenon.

The predicted behavior of a vibrating soil-foundation system is well supported by the available experimental evidence. An evaluation of experimentally determined amplitude-frequency response curves and phase angle-frequency curves support, furthermore, the validity of the proposed mathematical model for cohesive soils. It is shown, that the soil mass vibrating in-phase with the foundation is considerably smaller than was previously expected. It should be noted, however, that this mathematical model is not applicable to foundations on sand. For this case, the resonance frequency and the loss coefficient, remain practically constant, independent of changes of the radius of the foundation or the contact pressure.

APPENDIX

Notation

The following letter symbols have been adopted for use in this paper:

C_s = static spring constant of rigid circular plate on elastic half-space or load-displacement relation of circular foundation on soil.

C_0 = experimentally determined constant used to express the nonlinearity of load-displacement relation of circular foundations on soil.

D_s = dissipated energy per cycle.

$F = F_0 e^{i(\omega t+\Phi)}$ = harmonic exciting force acting on plate or foundation.

F_0 = amplitude of exciting force acting on plate or foundation.

$F_s = f(y)$ = nonlinear force-displacement function.

$\bar{F} = \bar{F}_0 e^{i(\omega t+\Psi)}$ = force acting between plate or foundation and half-space or subsoil.

$\bar{F}_0$ = force amplitude acting between plate or foundation and half-space or subsoil.

G = shear modulus of elastic half-space.

G_s = dynamic shear modulus of half-space.

$S = \bar{F}_0/y_0$ = dynamic stiffness.

U = stored energy.

U_s = energy required for the deformation of the half-space.

$a_0 = r_0\omega\sqrt{\rho/G_s}$ = frequency factor.
$a_{0r} = r_0\omega_0\sqrt{\rho/G_s}$ = frequency factor at resonance.
$\bar{a}_0 = (r_0/v_s)\sqrt{C_s/m_0} = (r_0/v_s)\sqrt{k_s g/\bar{p}}$.
b = damping constant of linear vibrating system.
$b_1 = 0.76$ = constant used to approximate function β.
$b_0 = m_0/\rho r_0^3$ = mass ratio.
C^* = experimental constant used to express the coefficient of subgrade reaction.
e = base of natural logarithms.
e_0 = eccentricity of rotating masses of vibrator.
f_1 = function of the frequency factor and Poisson's ratio.
$f_{10} = \lim_{a_0 \to 0} f_1$
f_2 = function of the frequency factor and Poisson's ratio.
g = acceleration of gravity.
$i = \sqrt{-1}$.
k_s = coefficient of subgrade reaction.
m_1 = eccentric mass of vibrator.
m_0 = mass of circular plate or foundation.
$\bar{m} = m_0 + m_s$ = effective vibrating mass.
m_s = participating soil mass.
n = experimental constant used to express the nonlinear load-displacement relation of circular foundations on soil.
$\bar{p}$ = average static contact pressure between foundation and subsoil.
p = experimental constant used to express the increase of the coefficient of subgrade reaction with an increase of the static contact pressure.
r_0 = radius of rigid circular plate or foundation.
r = experimental constant used to express the increase of the stiffness of soil with depth below ground level.
t = time.
v_s = shear wave velocity of soil.
v_c = compression wave velocity of soil.
y = displacement of plate or foundation.
y_0 = displacement amplitude of plate or foundation.
$\ddot{y}$ = acceleration of plate or foundation.
y_{0s} = displacement of foundation due to static load.
y_{0r} = displacement amplitude of plate or foundation at resonance.
Φ = phase angle between exciting force and displacement of plate or foundation.
Ψ = phase angle between force acting between the plate and the half-space and the resulting displacement.

Ψ_0 = specific damping capacity of soil.
$\alpha = f_1 f_{10}/(f_1^2 + f_2^2)$ = function expressing the inertia effect of the half-space on the restoring force.
$\alpha_0 = \alpha(a_{0r})$.
$\beta = f_2 f_{10}/(f_1^2 + f_2^2)$ = function expressing energy losses due to wave propagation.
γ = density of half-space or soil.
ε = constant used to approximate function α.
η = loss coefficient of soil.
$\eta_s = D_s/2\pi U_s$ = loss coefficient of vibrating plate or foundation.
ν = Poisson's ratio of half-space or soil.
ρ = mass density of half-space or soil.
ω = angular or circular frequency of vibrating system.
ω_0 = angular resonance frequency.
* The asterisk is used as a superscript to designate fixed known or experimentally determined quantities.

REFERENCES

1. Reissner, E., Stationäre, axial symmetrische, durch eine schüttelnde Masse erregte Schwingungen eines homogenen elastischen Halbraumes, Ing. Archiv., *7*, 1963, pp. 381–396.
2. Sechter, O. J., Sbornik Trudov, Vibracii Sooruzenij i Fundamentov, No. 12, Strojevojenmorizdat, Moskva, 1948, pp. 72–83.
3. Sung, T. Y., Vibrations in Semi-infinite Solids due to Periodic Surface Loading, Symposium on Dynamic Testing of Soils, ASTM Special Technical Publication No. 156, 1953, pp. 35–63.
4. Bycroft, G. N., Forced Vibrations of a Rigid Circular Plate on a Semi-infinite Elastic Space and on an Elastic Stratum, Phil. Trans. of the Royal Soc. of London, Series A, *248*, Math. and Phy. Sci., 1956, pp. 327–368.
5. Novák, M., Über die Nichtlinearität der Verticalschwingungen von starren Körpern auf dem Baugrunde, Acta Technica, Rocnik *2*, Nakladatelstvi CSAV, Praha II, CSR, 1957, pp. 365–409 and 456–492.
6. Novák, M., The Vibrations of Massive Foundations on Soil, International Association of Bridge and Structural Engineering, *XX*, 1960, pp. 263–281.
7. Ehlers, G., Der Baugrund als Federung in schwingenden Systemen, Beton und Eisen, *41*, 1942, pp. 197–203.
8. Pauw, A., A Dynamic Analogy for Foundation-Soil Systems, Symposium on Dynamic Testing of Soils, ASTM Special Technical Publication No. 156, 1953, pp. 90–112.
9. Balakrishna Rao, H. A. and Nagaraj, C. N., A New Method for Predicting the Natural Frequency of Foundation-Soil Systems, The Structural Engineer, *38*, 1960, pp. 310–316.
10. Bernhard, R. K. and Finelli, J., Pilot Studies on Soil Dynamics, Symposium on Dynamic Testing of Soils, ASTM Special Technical Publication No. 156, 1953, pp. 211–253.
11. Timoshenko, S. and Goodier, J. N., *Theory of Elasticity*, McGraw-Hill Book Company, Inc., 1951.
12. Lorenz, H., Neue Ergebnisse der dynamischen Baugrunduntersuchung, Zeitschrift Verein Deutscher Ingenieure, *79*, 1934, pp. 379–385.
13. Heukelom, W., Analysis of Dynamic Deflexions of Soils and Pavements, Geotechnique, *XI*, 1961, pp. 224–243.

14. Heukelom, W., Investigation of the Mechanical Elements Governing the Stiffness of Road Constructions, Koninklijke/Shell-Laboratorium, Amsterdam, Report No. M-23020, 1957.
15. Weissmann, G. F. and Hart, R. R., Damping Capacity of Some Granular Soils, ASTM Special Techn. Publication No. 305, 1961, pp. 45–54.
16. Barkan, D. D., *Dynamics of Bases and Foundations*, McGraw-Hill Book Company, Inc., 1960.
17. Weissmann, G. F., Determination of the Coefficient of Subgrade Soil Reaction, Materials Research and Standards, *5*, No. 2, 1965, pp. 71–75.
18. Weissmann, G. F. and White, S. R., Small Angular Deflexions of Rigid Foundations, Geotechnique, *11*, 1961, pp. 186–201.
19. Wilson, S. D. and Sibley, E. A., Ground Displacements Resulting from Air-Blast Loadings, Proc. ASCE, *88*, No. SM6, 1962, pp. 1–32.
20. Whitman, R. V., Effects of Viscosity and Inelasticity upon Stress Waves through Confined Soil, Shock, Vibration and Associated Environments, Bulletin No. 32, August, 1963, Protective Construction, Part III, pp. 107–123.
21. Fry, Z. B., Development and Evaluation of Soil Bearing Capacity Foundations of Structures; Field Vibratory Tests Data, Waterways Experiment Station, Technical Report No. 3-632, Report 1, 1963.
22. Converse, F. J., Compaction of Sand at Resonance Frequency, Symposium on Dynamic Testing of Soils, ASTM Spec. Techn. Publication No. 156. 1953, pp. 124–137.
23. Lorenz, H., *Grundbau Dynamik*, Springer Verlag, 1960.
24. Tschebotarioff, G. P., Performance Records of Engine Foundations, ASTM Spec. Techn. Publication No. 156, 1953, pp. 163–173.
25. Tschebotarioff, G. P., *Soil-Mechanics, Foundations, and Earth Structures*, McGraw-Hill Book Company, Inc., 1951.